Chapter IV

Results and Discussion

Contents

4.1 Expression of enzymes and androgen receptor in human hair dermal papilla cells

The effect of androgens on hair growth is exerted through interactions with the 5α-R and AR within HHDPCs **(Figure 5)**. HHDPCs are the main regulator of hair growth and without which the hair follicle does not exist. In addition, it is the only type of cell in the hair follicle that is the site of androgens action and expresses 5α-R [1, 9, 23]. As the presence of both the enzymes and the receptor in HHDPCs was important for this study, their expressions were evaluated. The RT-PCR analysis revealed that the genes of Type 1 enzyme, 5α-R1 and AR, were expressed in passages 2, 4, 5 and 6 of HHDPCs, while the Type 2 gene, 5α-R2 was not expressed in any of the passages **(Figure 7)**. In order to observe the possible products produced from the susbstrate, T, HHDPCs were also tested for the expression of aromatase and HSD17β2 which produces estradiol and androstenedione, respectively **(Figure 4)**. The RT-PCR results revealed that T will only be converted to 5α-DHT as both aromatase and HSD17β2 were not expressed in any of the passages within HHDPCs. β-actin, an internal control, was constantly expressed in all passages.

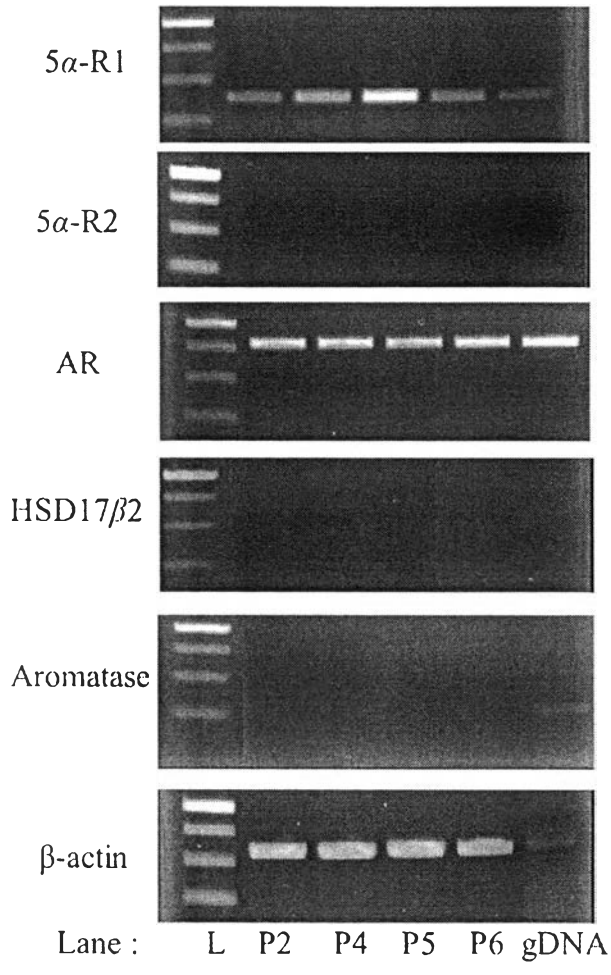

Figure 7. RT-PCR showing the expression of 5α-Rs, AR, HSD17β2 and aromatase in HHDPCs. A 1% agarose gel showing, from the top, the expression of 5α-R1 (5α-reductase type 1, 380 bp), 5α-R2 (5α-reductase type 2, 440 bp), AR (androgen receptor, 811 bp), HSD17β2 (17β-hydroxysteroid dehydrogenases type 2, 804bp), aromatase (1000bp), and β-actin (584 bp) within passages 2, 4, 5 and 6 of HHDPCs. The 1-kb DNA ladder (L) shows the band sizes of 1 kb and 750, 500 and 250 bp from top-down.

The expressions of all the proteins were consistent with the previously reported results [6, 8, 38-39, 58-60]. The results confirmed the suitability of HHDPCs to be used in cell-based study for the identification of new 5α-R1 inhibitors specifically for treating AGA. In addition, the presence of AR, make the cells compatible for studying the potential anti-androgenic activity of the 5α-R1 inhibitors.

4.2 Human hair dermal papilla cell-based assay system

Cell-based assay was chosen over cell-free assay, where the 5α-R enzyme has been reported to be isolated from the rat liver [17, 34, 50], prostate [14, 44], epididymis [18] or the human prostate [15], as the latter does not mimic the actual conditions of the enzymes and does not take into account the toxicity of the test compounds [19]. In addition, the reliability of the cell-free system is presumably low because the sequence similarities between the 5α-R1 and 5α-R2 from rats and humans is only 61% and 75% [6], respectively, which might affect the nature of active site formation and hence the activity. Also, two isoforms of the enzymes, 5α-R1 and 5α-R2, are specifically distributed in different organs within the human body [6], and therefore testing the enzyme isolated from the human prostate [15] might not be relevant to the type of enzyme present in human hair cells.

In order to obtain the cell-based assay system relevant for hair loss, it is more appropriate to use hair cells than transfected rat [19] or insect [16] cell lines. These cell lines of rat, insect and human possess different levels of toxicity tolerance to the test compounds, such that a potent concentration of 5α-R inhibitor for the rat or insect cell line might be toxic to human hair cells. Hair comprises of at least fifteen distinct types of cells where the HHDPCs are primary cells that regulates hair growth and is the only site of androgens action [1, 9, 22] and expressed 5α-R1. Therefore, these cells were used as a model for the identification of new, potent 5α-R1 inhibitors for the treatment of AGA

4.2.1 Cytotoxicity of testosterone on human hair dermal papilla cells

To obtain a suitable starting concentration for treating the HHDPCs, the T cytotoxicity was evaluated at various concentrations, ranging from the highest solubility of T in cell culture medium (i.e., 10^{-4} M) to its lowest physiological concentration of 10^{-8} M. All the concentrations of T were found to be non-toxic as the cell viability was close to 100% **(Figure 8)**.

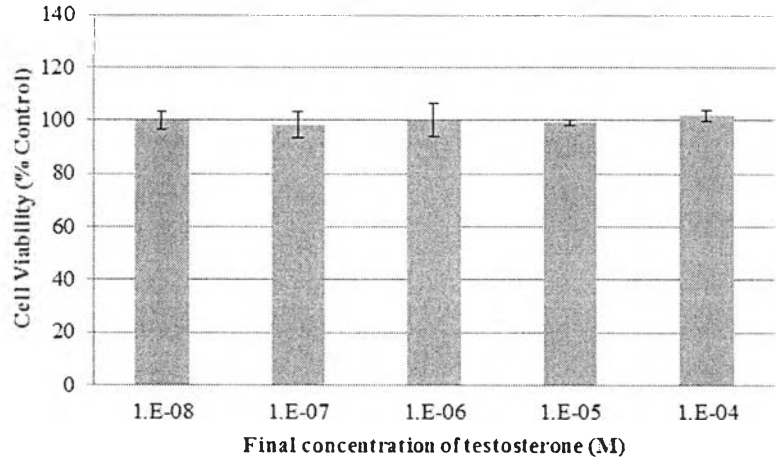

Figure 8. Cytotoxicity of T on HHDPCs

Therefore, all the five concentrations were used to treat HHDPCs in order to visualize the enzyme activity on the TLC plate using a newly developed non-radioactive TLC detection technique. In order to quantitate the 5α-DHT produced, first an image of the developed and derivatized plate was taken at 366 nm and then the 5α-DHT band was quantitated using an image analyzing program, Quantity One (Bio-rad, USA) instead of scanning it using a TLC scanner. This is because an instrumental error was found when the plates with the enzymatic reactions were scanned. However, this error was not observed on the TLC plate containing different concentration of 5α-DHT alone which was conducted to obtain the standard curve. Therefore, an imaging detection technique was developed to quantitate the amount of 5α-DHT produced which gave a similar correlation coefficient (R^2) as the scanner (Figures 9A and 9B).

A

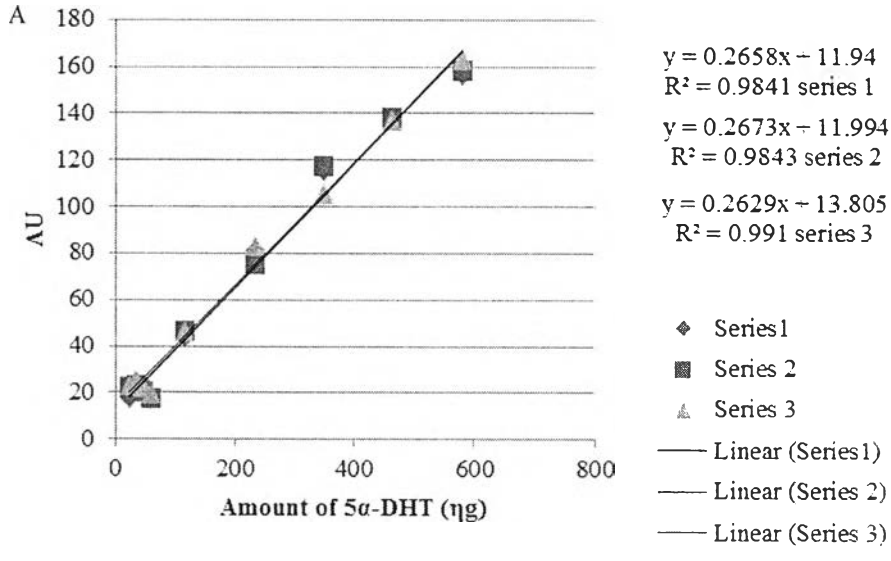

B

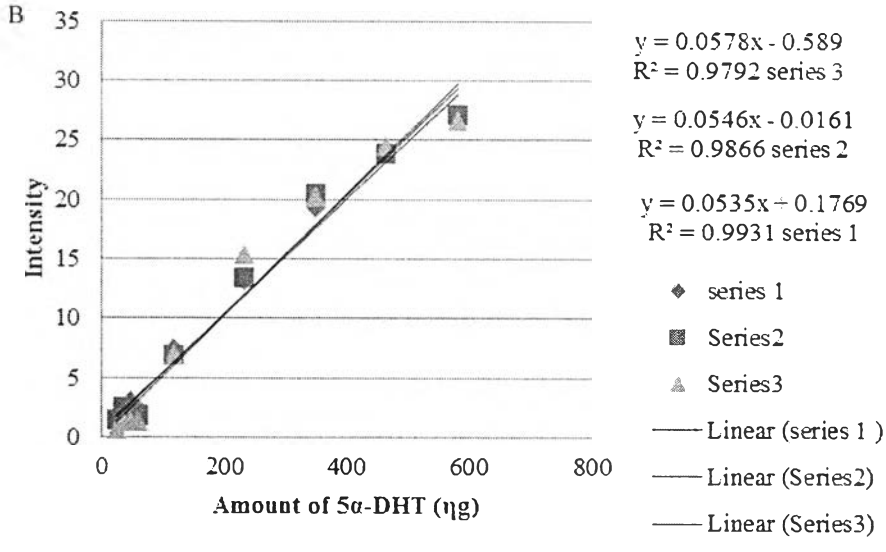

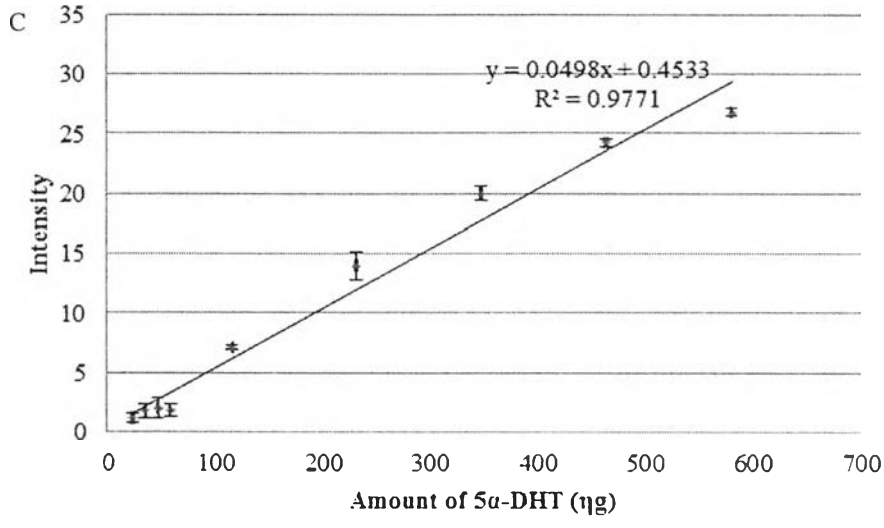

Figure 9. Standard curve of 5α-DHT, quantitated using (A) TLC scanner at 366 nm (B) image analyzing program, Quantity One. (C) Average standard curve of 5α-DHT quantitated using image analyzer

The average R^2 value of both the quantification technique was 0.986. The average standard curve of 5α-DHT quantitated using image analyzer gave the limit of detection (LOD) of 1.36, calculated from 3*y-intercept value and limit of quantification (LOQ) of 4.53, calculated from 10* y-intercept **(Figure 9C)**.

This non-radioactive TLC detection technique is much safer and feasible as compared to the present available system which uses complicated detectors, such as the radioactive image analyzer [17, 44], TLC radioactive scanners [19], HPLC radioactive detectors [16] or measuring the decrease in radiolabelled T concentration at 254 nm using HPLC [14-15, 18, 50].

4.2.2 Optimization of the assay system

All the five final concentrations were used to treat HHDPCs in the 96-well plate for 24 and 48 hours before the substrate, T, and the product, 5α-DHT, were isolated from the cell culture medium. The 5α-DHT produced by the 5α-R1 expressed in HHDPCs **(Figure 7)** was clearly detectable on the TLC plate when the cells were treated with the final concentration of 10^{-4} M T for 48 hours **(Figure 10A)** and was not clearly detectable at 24 hours **(Figure 10B)** using the developed non-radioactive TLC detection technique.

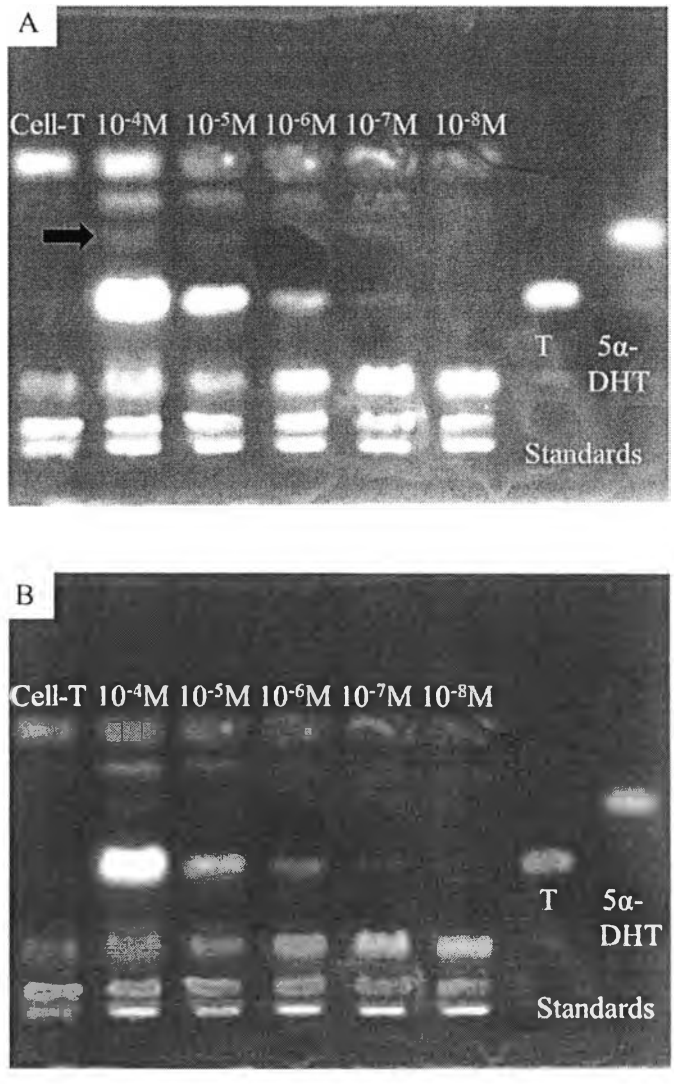

Figure 10. Results from the enzymatic reaction using HHDPC-based assay after (A) 48 hours and (B) 24 hours of treatment with the final five concentrations of T. The negative control (Cell-T) is shown on the left-hand side of the plate.

4.2.3 Inhibitory activity of dutasteride on human hair dermal papilla cells

The optimized system was first tested using a well-known 5α-R1 inhibitor, dutasteride, as a positive control. To determine the starting concentration to test for the inhibitory activity, the cytotoxicity of dutasteride on HHDPCs was carried out using the PrestoBlue® cell viability reagent. Dutasteride exhibited toxicity (i.e., cell viability less than 85%) above the final concentration of 10 μg/ml **(Figure 11A)** while

showing complete inhibition at this concentration compared to the internal control (Cell+T) **(Figure 11B)** with an IC_{50} value of 0.005 µg/ml or 9.7 nM **(Figure 11C)**.

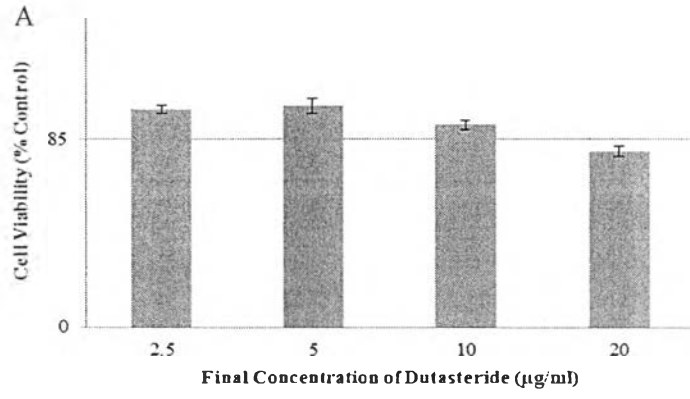

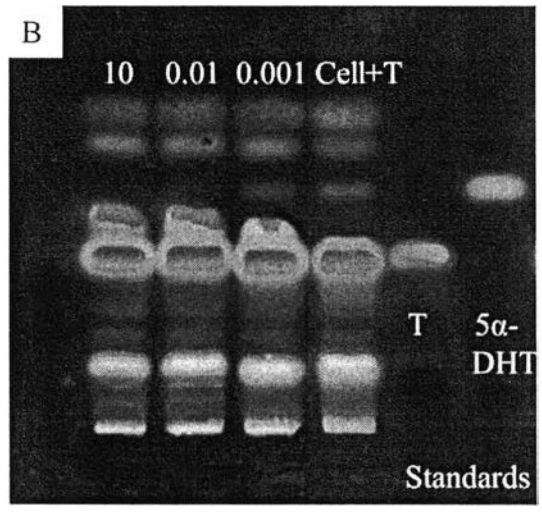

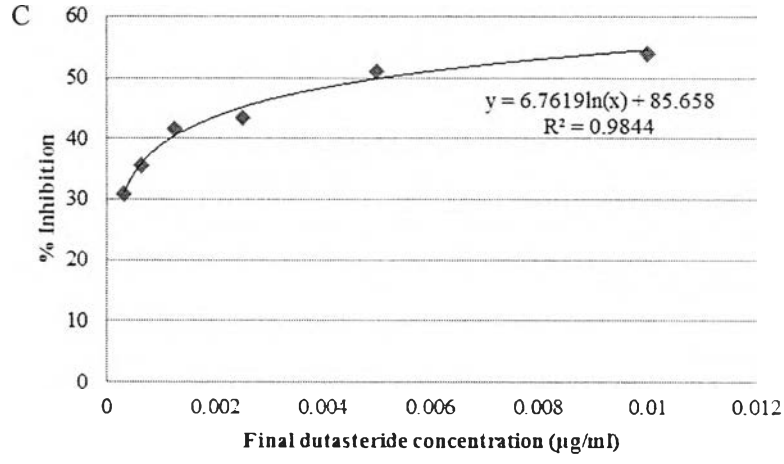

Figure 11. (A) Cytotoxicity of dutasteride at 20, 10, 5 and 2.5 µg/ml. (B) Inhibitory activity of dutasteride at 0.001, 0.01 and 10 µg/ml on HHDPCs. The internal control is referred as Cell+T. (C) IC_{50} curve of dutasteride.

4.3 Cytotoxicity of methanolic plant extracts on human hair dermal papilla cells

To obtain a suitable starting concentration for screening methanolic plant extracts for the 5α-R1 inhibitory activity, the cytotoxicity of each plant extract on HHDPCs at various concentrations was subsequently tested using the PrestoBlue® cell viability reagent. The results showed that each extract, at their final concentrations, exhibited different toxic level on the cells **(Figure 12)**. The plant extracts of DM and SG were the most toxic above the final concentration of 2.5 µg/ml, followed by the ST, ASC and DP extracts, which showed toxicity above 5 µg/ml **(Figure 12A)**. The other extracts with moderate toxicity above 10 µg/ml were SD, OM, AM, CLO and, OI **(Figure 12B)**, while the remaining extracts, including AG, AS,ASHE, ASHO, BA, BC, BM, BM2, BM3, CA, CD, CH, CI, CL, CR, CRB, CT, DE, KG, LH, MC, MF, MM, PA, RH, SV, TF, TH, TM, ZL, and ZO showed no toxicity even at 20 µg/ml **(Figure 12C-12F)**. Based on these results, the highest final non-toxic concentration of each extract, summarized in **Table 8**, showing cell viability greater than 85% was used for the subsequent inhibitory activity test.

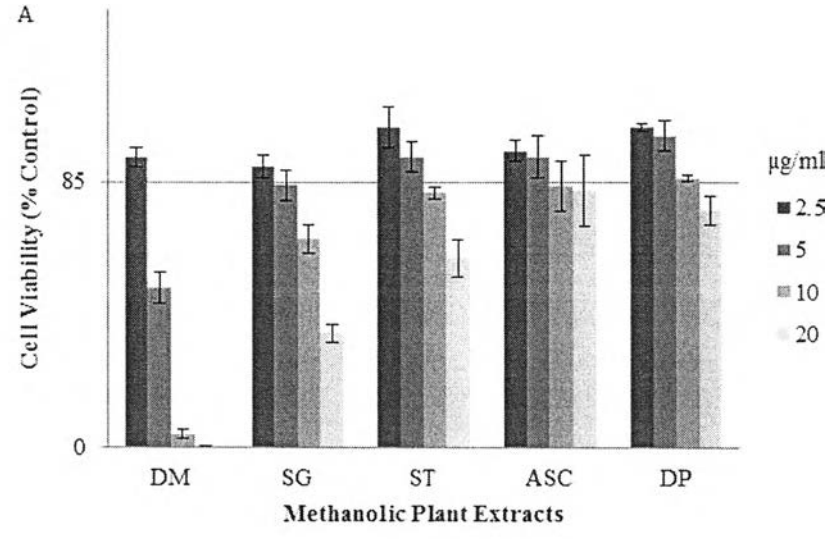
A
Cell Viability (% Control)
85
0
DM
SG
ST
ASC
DP
Methanolic Plant Extracts
µg/ml
2.5
5
10
20

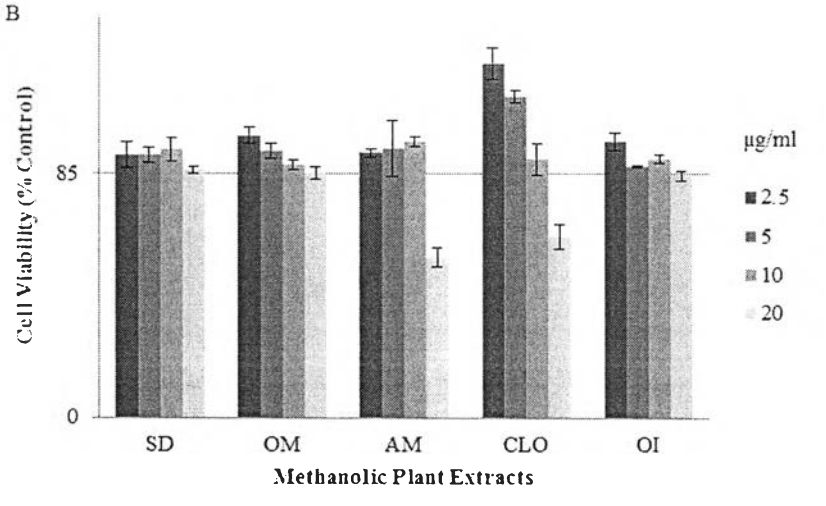
B
Cell Viability (% Control)
85
0
SD
OM
AM
CLO
OI
Methanolic Plant Extracts
µg/ml
2.5
5
10
20

C

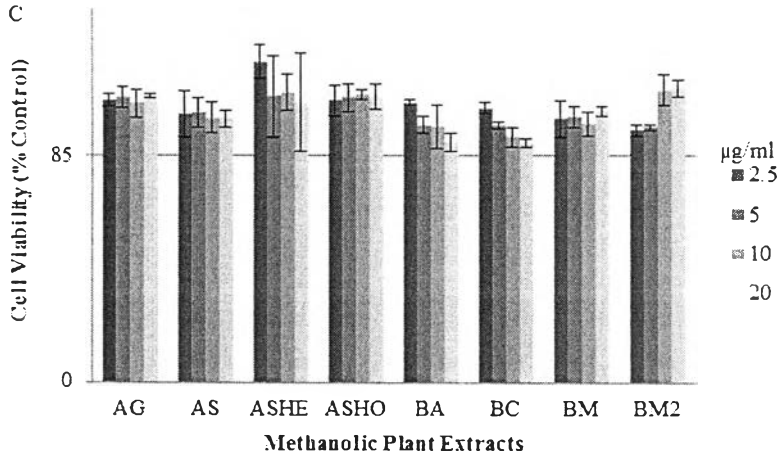
Cell Viability (% Control)
85
0
AG
AS
ASHE
ASHO
BA
BC
BM
BM2
Methanolic Plant Extracts
µg/ml
2.5
5
10
20

D

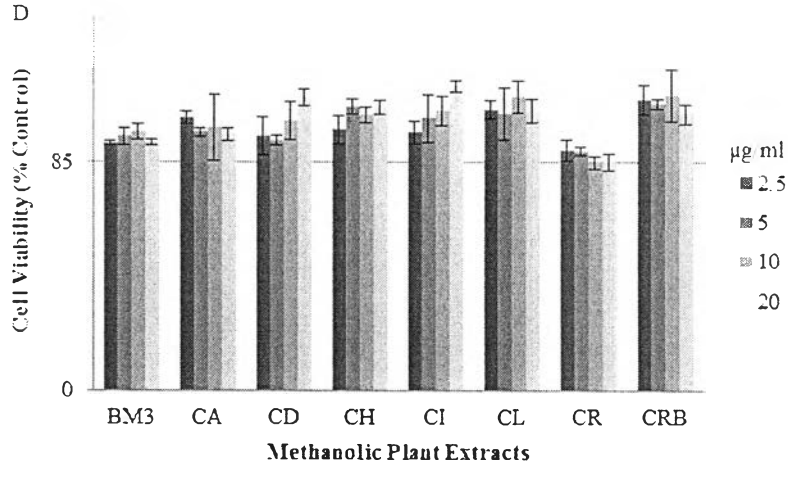
Cell Viability (% Control)
85
0
BM3
CA
CD
CH
CI
CL
CR
CRB
Methanolic Plant Extracts
µg/ml
2.5
5
10
20

E

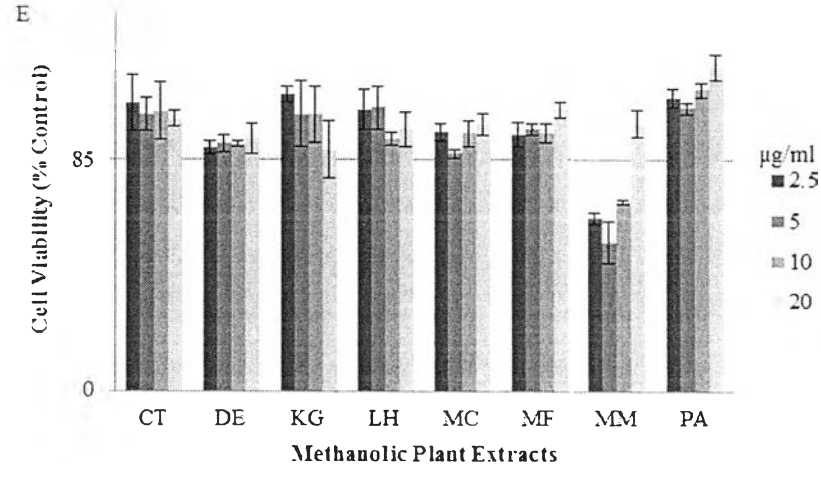
Cell Viability (% Control)
85
0
CT
DE
KG
LH
MC
MF
MM
PA
Methanolic Plant Extracts
µg/ml
2.5
5
10
20

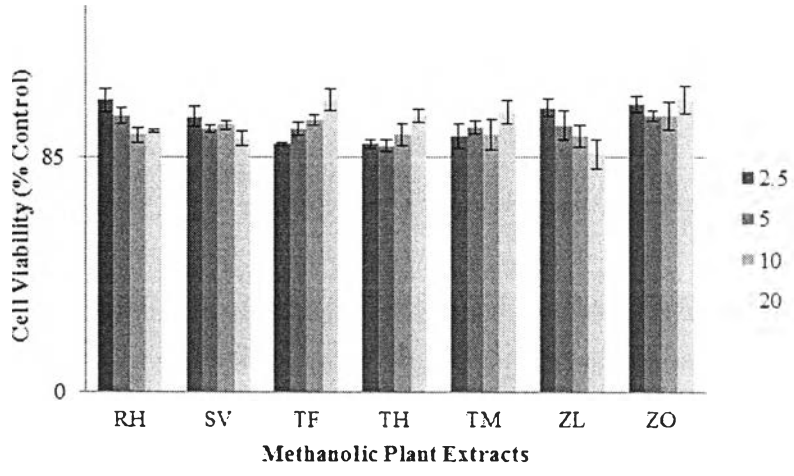

Figure 12. Results on the cytotoxicity of methanolic plant extracts exhibiting (A) highest (greater than 2.5 and 5 µg/ml), (B) moderate (greater than 10 µg/ml) and (C-F) no (20 µg/ml) toxicity

4.4 Identification of plant extracts possessing 5α-R1 inhibitory activity using human hair dermal papilla cell-based assay system

As previously discussed, AGA is caused due to the over-production of 5α-DHT by the 5α-R [1-6]. Thus, one potential mechanism for reducing the effect of this androgen is to inhibit this enzymatic reaction. The methanolic plant extracts at their highest final non-toxic concentrations were tested for the 5α-R1 inhibitory activity using the optimized HHDPC-based assay system. As shown in **Figure 13A-13D**, each lane represents the inhibitory potential of each extract. The lane "Cell+T" was the internal control representing the conversion of T to 5α-DHT while the lane "Cell-T" was the negative control. Among all the extracts screened, the plant extracts of MM, CLO, BM, DM, and OM, showed only 10-15% inhibition while the extracts of KG and CH showed approximately 20% inhibition. The highest and the only significant inhibitory activity was observed from the crude extract of AM at the final concentration of 10 µg/ml through the reduction in 5α-DHT production by more than 50% **(Table 8)** with the IC_{50} value of 9.21 µg/ml **(Figures 14)**. The viability of the attached treated cells in the 96-well plate was 100.5 ± 2.02% (n=3), confirming the positive effect of AM extract. Therefore, the crude extract of *Avicennia marina* (AM) was used for subsequent studies.

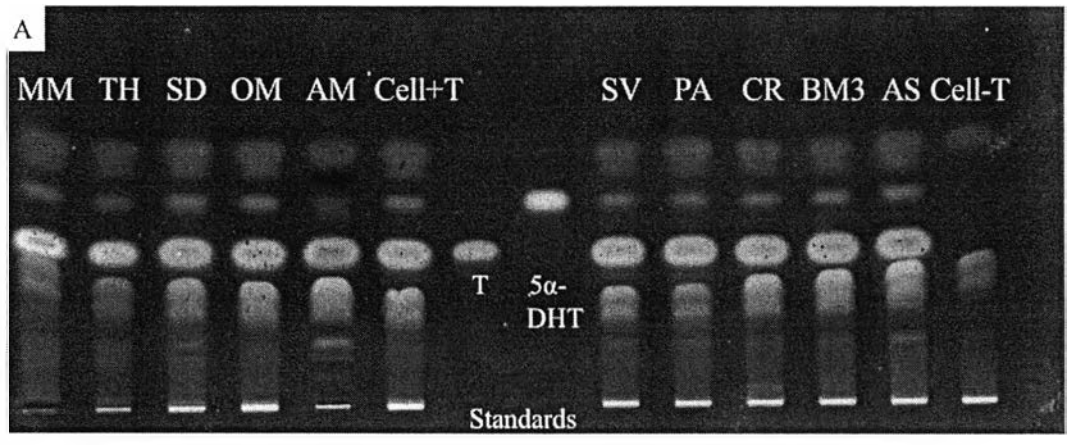
A
MM TH SD OM AM Cell+T
SV PA CR BM3 AS Cell-T
T
5α-
DHT
Standards

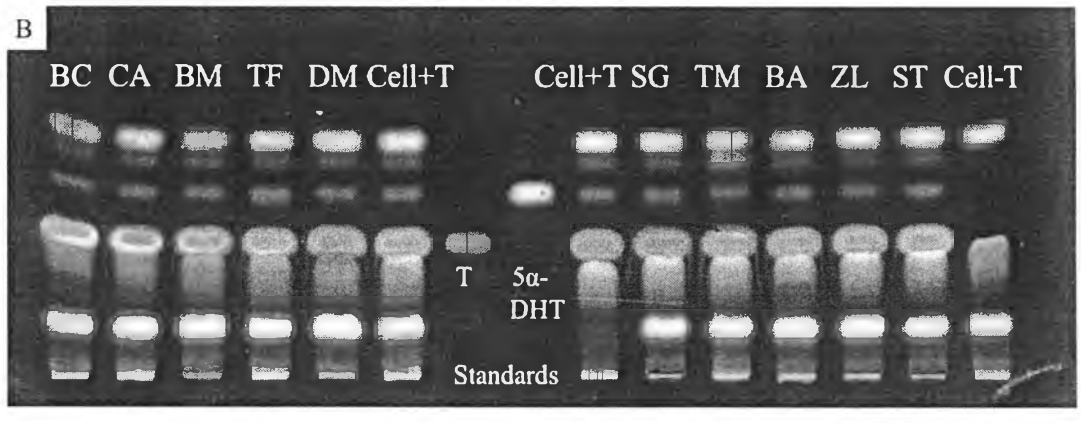
B
BC CA BM TF DM Cell+T
Cell+T SG TM BA ZL ST Cell-T
T
5α-
DHT
Standards

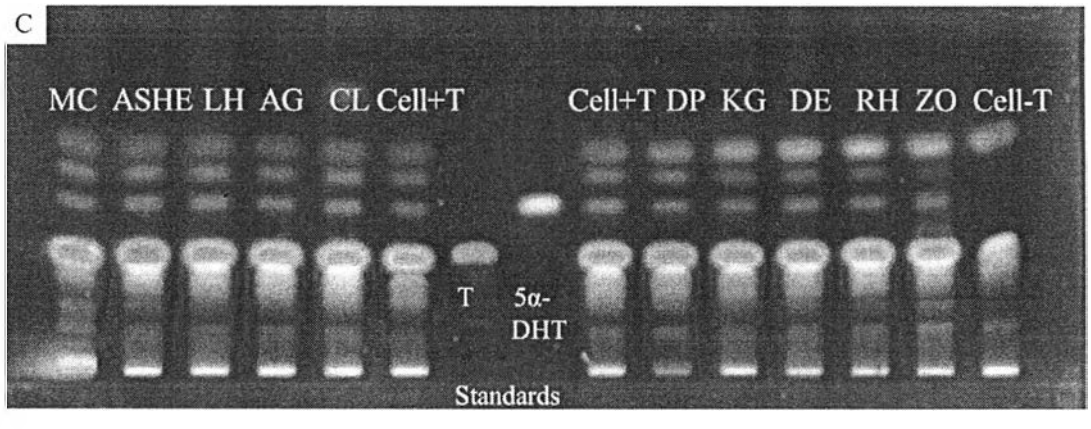
C
MC ASHE LH AG CL Cell+T
Cell+T DP KG DE RH ZO Cell-T
T
5α-
DHT
Standards

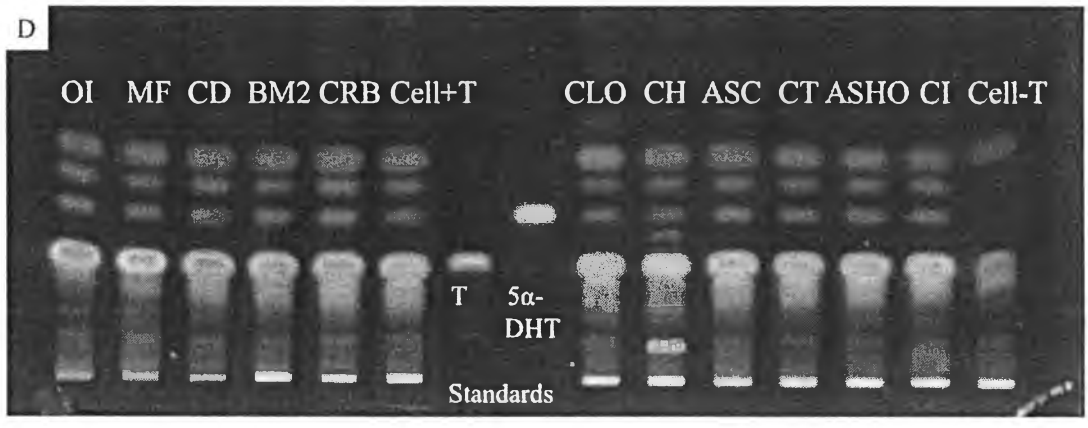

Figure 13. 5α-R1 inhibitory activity of the methanolic plant extracts at their highest final non-toxic concentrations in HHDPC-based assay using a non-radioactive TLC detection technique. Each lane shows the inhibitory activity for individual test compounds. The internal (Cell+T) and negative (Cell-T) control are shown in the middle and right-hand side of the plates, respectively.

(A) *Micromelum minutum* – MM, *Tarenna hoaensis* – TH, *Scoparia dulcis* – SD, *Olendra musifolia* – OM, *Avicennia morina* – AM, *Salacia verrucosa* – SV, *Pterygota alata* – PA, *Crotalasia retusa* – CR, *Bacopa monnerii* – BM3, *Afgekia sericea*- AS

(B) *Barleria cristata* – BC, *Centella asiatica* – CA, *Butea monosperma* – BM, *Tarenna fragans* – TF, *Diospyros mollis* – DM, *Seena garrethiana* – SG, *Telosma minor* – TM, *Balanophora abbreviate* – BA, *Zanthoxylum limonella* –ZL, *Senna timoriensis* – ST

(C) *Maclura cochinchinen* – MC, *Alternanthera sessilis* (hexane extract)- ASHE, *Leersia hexandra* – LH, *Alpinia galangal* – AG, *Citrus limonum* – CL, *Dalbergia parviflora* – DP, *Kaempferia galangal* – KG, *Derris elliptica* – DE, *Randia horrida* – RH, *Zingiber officinale* – ZO

(D) *Ochna integerrima* – OI, *Myristica fragrans* – MF, *Caesalpiria digyna* – CD, *Bauhinia malabarica* – BM2, *Citrus reticulata blanco*- CRB, *Curcuma Longa* – CLO, *Citrus hystix* – CH, *Alternanthera sessilis* (dichloromethane extract)- ASC, *Clitoria ternatea* , *Alternanthera sessilis* (water extract) – ASHO, *Chrysanthemum indicum* – CI

Table 8

Relative 5α-DHT produced by HHDPCs after treating with the final non-toxic concentrations of methanolic plant extracts

Medicinal plant	Abbreviation	Final concentration (μg/ml)	Relative 5α-DHT production
*Avicennia marina**	AM	10	0.48 ± 0.03
Kaempferia galangal	KG	20	0.79 ± 0.18
Citrus hystix	CH	20	0.81 ± 0.06
Micromelum minutum	MM	20	0.84 ± 0.03
Curcuma longa	CLO	10	0.86 ± 0.01
Butea monosperma	BM	20	0.87 ± 0.07
Diospyros mollis	DM	2.5	0.89 ± 0.04
Olendra musifolia	OM	10	0.90 ± 0.09
Maclura cochinchinen	MC	20	0.91 ± 0.05
Myristica fragrans	MF	20	0.91 ± 0.14
Barleria cristata	BC	20	0.91 ± 0.20
Balanophora abbreviate	BA	20	0.92 ± 0.04
Alpinia galangal	AG	20	0.93 ± 0.03
Randia horrida	RH	20	0.93 ± 0.15
Clitoria ternatea	CT	20	0.94 ± 0.01
Centella asiatica	CA	20	0.94 ± 0.01
Derris elliptica	DE	20	0.94 ± 0.12
Ochna integerrima	OI	10	0.96 ± 0.02
Telosma minor	TM	20	0.96 ± 0.05
Zanthoxylum limonella	ZL	20	0.96 ± 0.13
Alternanthera sessilis	ASC[b]	5	0.99 ±0.02
Salacia verrucosa	SV	20	1.01 ± 0.07
Crotalasia retusa	CR	20	1.01 ± 0.13
Bauhinia malabarica	BM2	20	1.02 ± 0.05
Senna timoriensis	ST	5	1.02 ± 0.19
Citrus limonum	CL	20	1.03 ± 0.11
Zingiber officinale	ZO	20	1.04 ± 0.13
Dalbergia parviflora	DP	5	1.04 ± 0.17
Afgekia sericea	AS	20	1.05 ± 0.03
Bacopa monnerii	BM3	20	1.05 ± 0.09
Chrysanthemum indicum	CI	20	1.05 ± 0.13
Leersia hexandra	LH	20	1.06 ± 0.02
Alternanthera sessilis	ASHE[c]	20	1.06 ± 0.12
Tarenna hoaensis	TH	20	1.07 ± 0.12
Pterygota alata	PA	20	1.10 ± 0.15
Alternanthera sessilis	ASHO[a]	20	1.12 ± 0.19
Scoparia dulcis	SD	10	1.16 ± 0.04

Table 8 (Cont.)

Relative 5α-DHT produced by HHDPCs after treating with the final non-toxic concentrations of methanolic plant extracts

Medicinal plant	Abbreviation	Final concentration (µg/ml)	Relative 5α-DHT production
Seena garrethiana	SG	2.5	1.16 ± 0.08
Caesalpiria digyna	CD	20	1.16 ± 0.15
Tarenna fragans	TF	20	1.17 ± 0.03
Citrus reticulata blanco	CRB	20	1.30 ± 0.02

a- Partitioned with water

b- Partitioned with dichloromethane

c- Partitioned with hexane

*- Statistically significant ($p<0.05$)

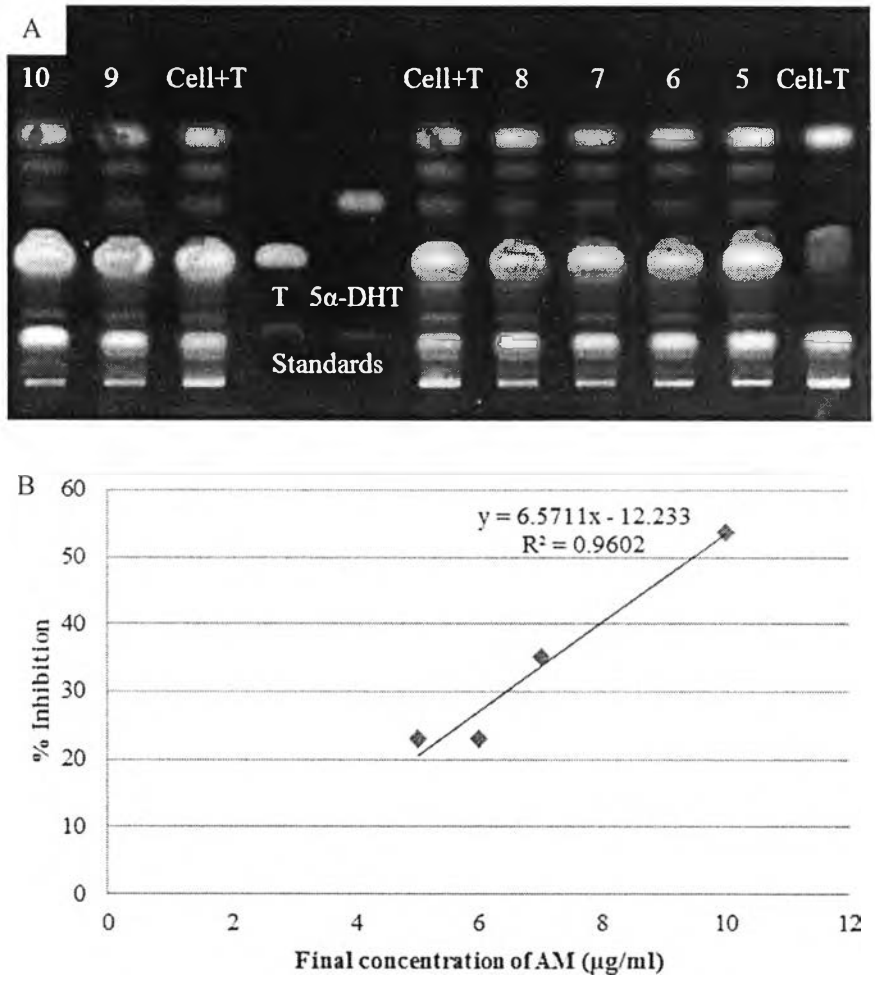

Figure 14. (A) TLC plate showing 5α-R1 inhibitory activity of AM at 10, 9, 8, 7, 6 and 5 µg/ml. The internal control (Cell+T) and negative control (Cell-T) are shown in the middle and right-hand side of the plate, respectively. (B) IC_{50} curve of AM.

4.5 Cytotoxicity of 5α-dihydrotestosterone on human hair dermal papilla cells

In order to obtain the potential of AM extract to overcome the effect of the much more potent androgen within HHDPCs, suitable treatment concentration of 5α-DHT is required. Therefore, the toxicity of 5α-DHT on HHDPCs was evaluated using the PrestoBlue® cell viability reagent. The results showed that HHDPCs were not toxic to all of the concentrations of 5α-DHT as the cell viability was close to 100% **(Figure 15)**. The highest final non-toxic concentration of 10^{-4} M 5α-DHT was the highest solubility in the cell culture medium and was chosen for testing the anti-androgenic activity of AM.

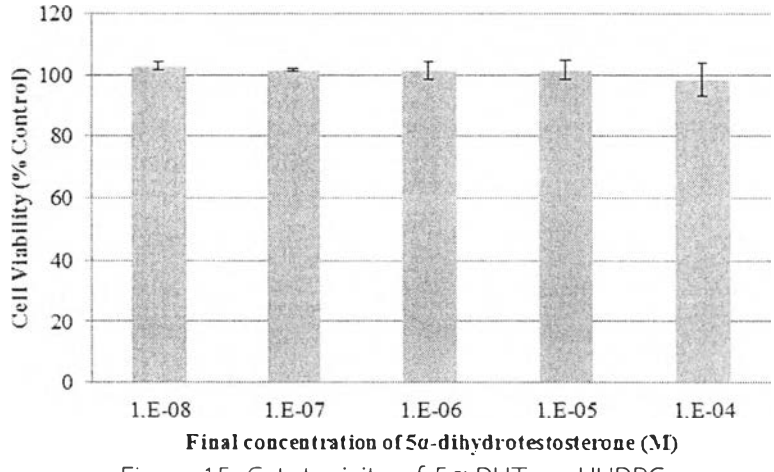

Figure 15. Cytotoxicity of 5α-DHT on HHDPCs

4.6 Anti-androgenic activity of *Avicennia marina* and dutasteride on human hair dermal papilla cells

Based on the mechanism of androgens action, a potent 5α-R inhibitor would lower the cellular level of 5α-DHT which would reduce the formation of the receptor-ligand complex, affecting the induction of androgen-sensitive genes of the growth factors expressed by HHDPCs. These growth factors include IGF-1, FGF-7, VEGF and HGF which are known to be localized in the DP compartment of the hair follicle and are responsible for the proliferation and differentiation of keratinocytes during the anagen phase of the hair cycle [23-24]. Therefore, the effects of AM extract, a potent 5α-R1 inhibitor, on the mRNA expression of these growth factors in androgens treated and un-treated HHDPCs was evaluated using RT-PCR. The result of the mRNA

expression was visualized on 1% agarose gels and the intensity of the bands **(Figure 16A)** indicated the expression level of each growth factor. The bands were quantitated relative to β-actin using ImageLab software **(Figure 16B)**. In the presence of 10^{-4} M T (lane 2), the expression level of FGF-7, VEGF and HGF decreased from 1.0 to 0.742, 0.493 and 0.02, respectively. However, a much more potent effect was observed when the cells were treated with 10^{-4} M 5α-DHT (lane 3) where the expression of FGF-7 and VEGF decreased to 0.574 and 0.402, respectively, and HGF was not expressed. In the presence of AM extract, an overcoming effect of 10^{-4} M T was observed through the up-regulation of all the three growth factors: FGF-7 from 0.742 to 1.038, HGF from 0.02 to 0.209 and VEGF from 0.493 to 1.035 (lane 5 compared with lane 2, Figure 16). A similar overcoming effect of AM was observed on cells treated with the more potent androgen, 5α-DHT, through the up-regulation of FGF-7 from 0.574 to 0.621 and VEGF from 0.402 to 0.649 (lane 6 compared with lane 3, Figure 16). AM exhibited a minimal overcoming effect on HGF in presence of 10^{-4} M 5α-DHT. In addition, it reduces the mRNA expression of HGF to 0.399 (lane 4 compared with lane 1, Figure 16) in absence of androgens. In presence of 10^{-4}M T, dutasteride exhibited an overcoming effect from 0.742 to 0.871 for FGF-7 and from 0.493 to 0.757 for VEGF (lane 8 compared to lane 2, Figure 16). A similar effect in presence of 10^{-4}M 5α-DHT was observed for FGF-7, from 0.574 to 0.848 and VEGF, from 0.402 to 0.586 (lane 9 compared to lane 3, Figure 16). However, dutasteride on its own exhibited down-regulation of FGF-7, VEGF and HGF growth factors from 1 to 0.841, 0.666, and 0, respectively (lane 7 compared with lane 1, Figure 16). Both the treated and un-treated HHDPCs did not express detectable amount of IGF-1.

A

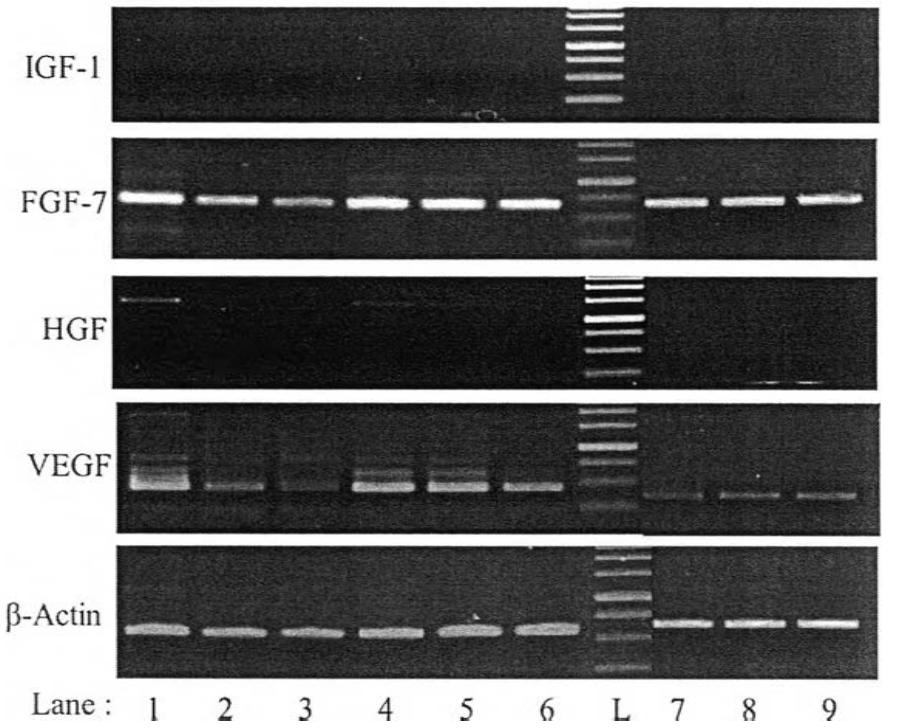

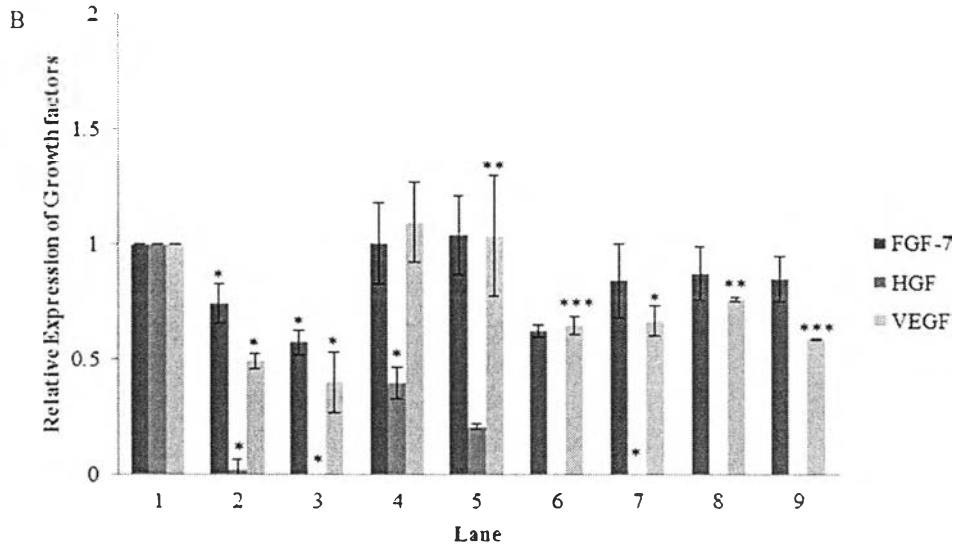

Figure 16. (A) RT-PCR and (B) relative levels of the mRNA expression of growth factors from androgens, AM and dutasteride treated and un-treated HHPDCs. Growth factors include IGF-1 (insulin-like growth factor 1, 361 bp), FGF-7 (fibroblast growth factor-7, 653 bp), HGF (hepatocyte growth factor, 1320 bp) and VEGF (vascular endothelial growth factor, 440 bp) while β-actin (584 bp) was used as an internal control. The 1-kb DNA ladder shows the sizes of 2, 1.5, and 1 kb and 750, 500 and 250 bp from top-down (lane L) and HHDPC treated with 1% DMSO (Lane 1), 10^{-4} M T (Lane 2), 10^{-4} M 5α-DHT (Lane 3), 10 µg/ml of AM (Lane 4), 10 µg/ml of AM and 10^{-4} M T (Lane 5) and 10 µg/ml of AM and 10^{-4} M 5α-DHT (Lane 6), 10 µg/ml of dutasteride (Lane 7), 10 µg/ml of dutasteride and 10^{-4} M T (Lane 8), 10 µg/ml of dutasteride and 10^{-4} M 5α-DHT (Lane 9). *- statistically significant compared to lane 1, **- statistically significant compared to lane 2, ***- statistically significant compared to lane 3 ($p<0.05$)

From the results obtained, it was found that AM significantly possess anti-androgenic activity through the up-regulation of VEGF in androgen-treated HHDPCs while down-regulating the expression of HGF in un-treated HHDPCs. Dutasteride also exhibited a similar significant anti-androgenic activity through the up-regulation of VEGF while it down-regulated the expression of HGF and VEGF growth factors in un-treated HHDPCs. As both AM and dutasteride showed similar properties, it might be possible that the decrease in 5α-DHT production led to the up-regulation of VEGF in androgen-treated HHDPCs. In addition, a significant increase in the expression of VEGF

was observed in presence of 5α-DHT, indicating that there might be other pathways through which AM and dutasteride interacts within HHDPCs.

4.7 Effect of androgens and *Avicennia marina* on the human hair dermal papilla cell's morphology

As AM exhibited molecular effect through a significant up-regulation of VEGF, its macroscopic effect on the HHDPCs' morphology was also evaluated. As shown in **Figure 17**, no morphologically effects such as changes in the size or shape of the cells were observed due to either the androgens, AM or their combinations. The direction of the cells doesn't signify any effect as in different well the cells orient in different ways. In addition, stained cells showed us that neither does the androgens nor the AM extract nor their combinations were toxic to the cells as they didn't exhibit white condensed nucleus in presence of Hoechst 33342 indicating apoptosis or red colored cells in presence of PI indicating necrosis. These results corresponds with our cytotoxicity results of T, 5α-DHT and AM extract which showed that all the concentrations used were non-toxic as the cells did not undergo either of the two types of cell death namely: apoptosis and necrosis. These results indicate that both the 5α-R1 inhibitory and anti-androgenic activities of AM are purely due to the active compounds present within the extract and are not false positive results.

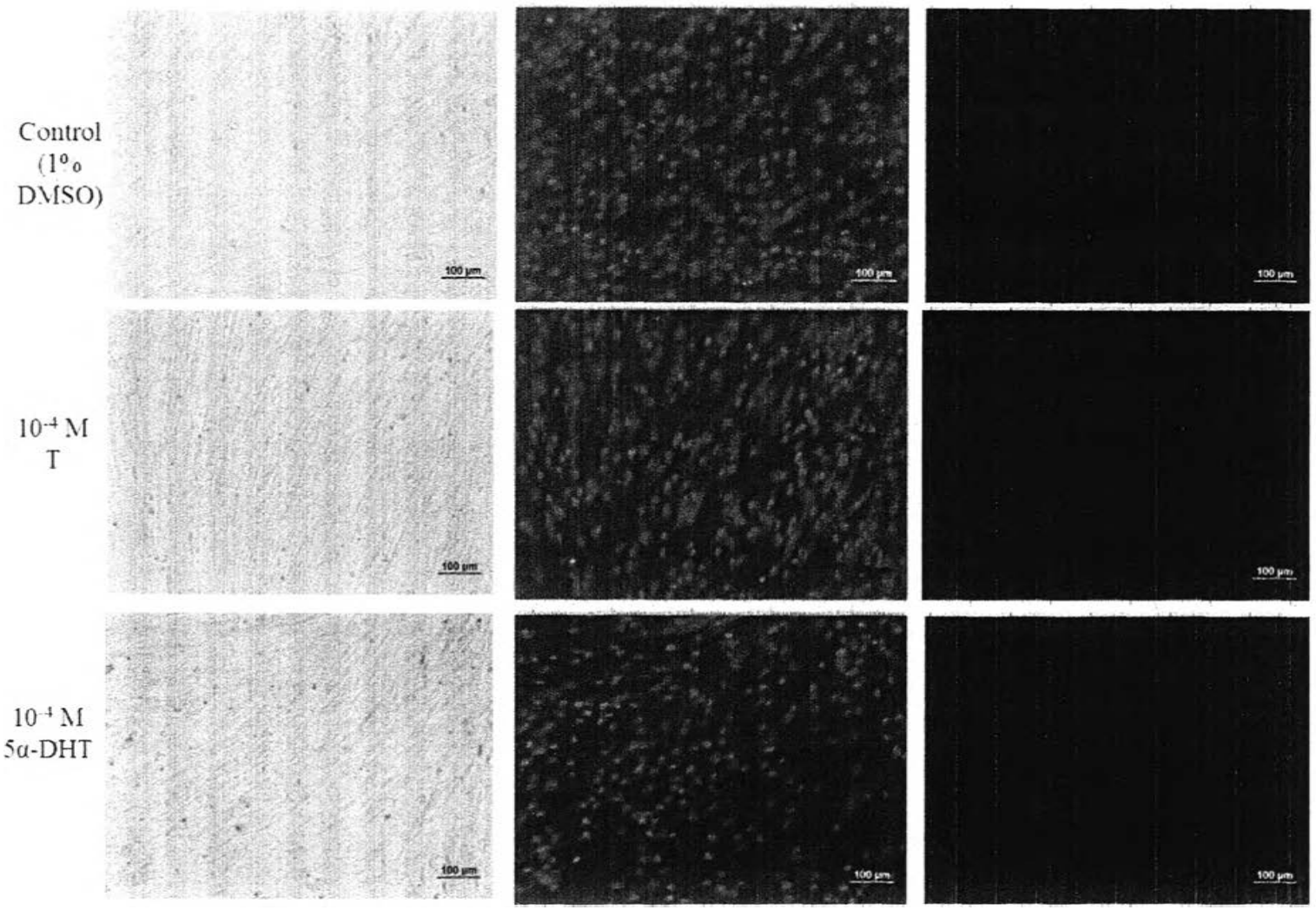

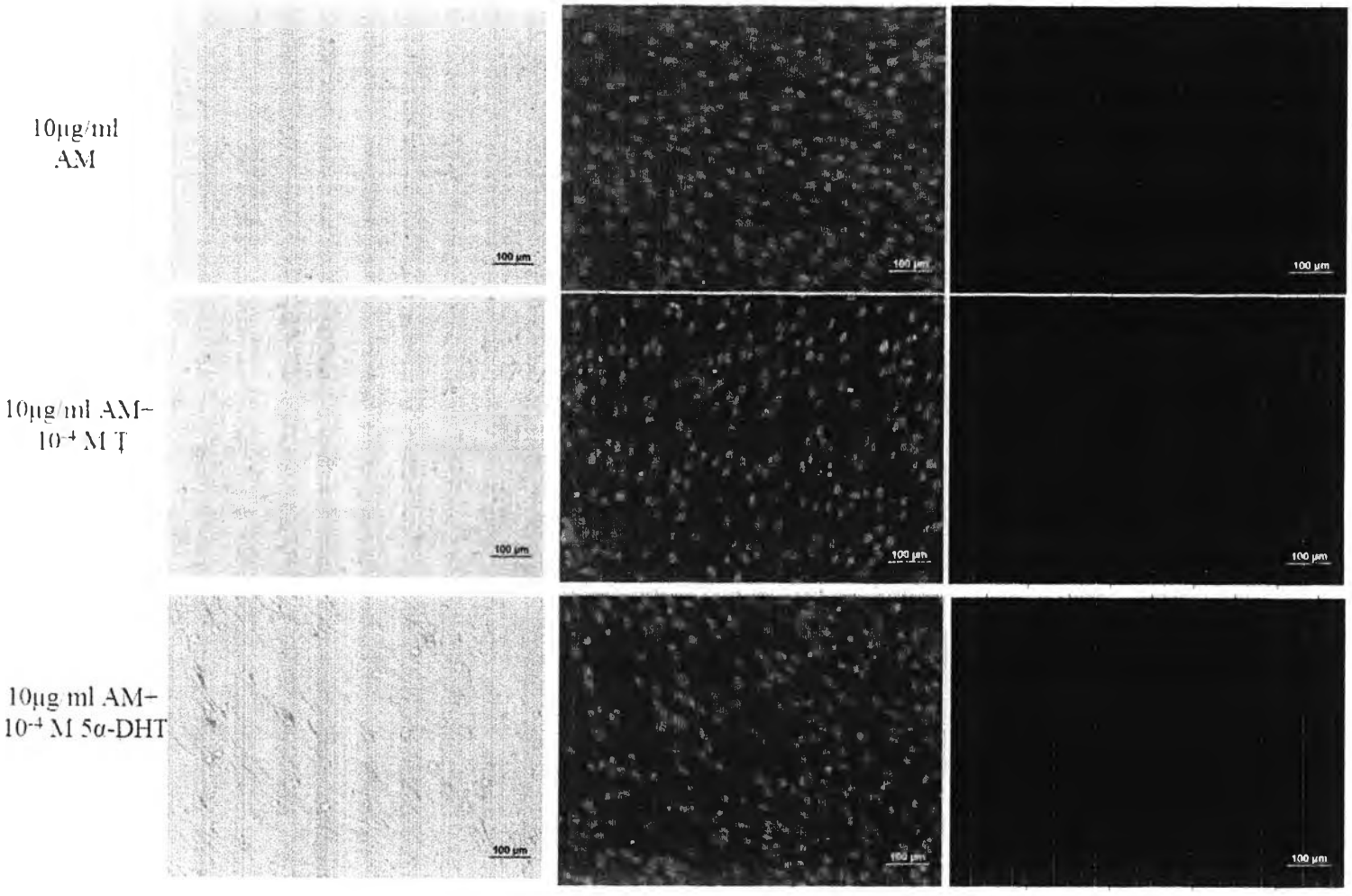

Figure 17. Results on the HHDPCs' morphology at 10X using phase contrast mode (left-hand side), Hoechst 33342 staining (middle) and Propidium iodide staining (right-hand side)

4.8 Thin layer chromatographic profile of *Avicennia marina*

AM, commonly known as gray or white mangrove, is a species of mangrove trees belonging to the Acanthaceae family and it has been traditionally used in Egypt to cure skin diseases [59]. Phytochemically, naphthalene derivatives, flavones, iridoid glucosides, prenylpropanoid glycosides, abietane ditrerpenoid glucosides, flavonoids terpenoids and steroids have been identified from various parts of AM [59]. Active compound(s) within the AM extract exhibiting 5α-R1 inhibitory activity might be in one of these natural product groups and in order to identify them, activity guided-fraction was carried out. Generally, column chromatography is used, however, multiple isolations are required for the isolation of active compounds and the compounds cannot be visualized for their purity. Therefore, TLC was used instead for the isolation, as it provides direct visualization of compounds at 254 and 366 nm. Firstly, the chemical complexity of AM extract **(Figure 18)** was observed at 254 **(Figure 18A)** and 366 nm **(Figure 18B)**.

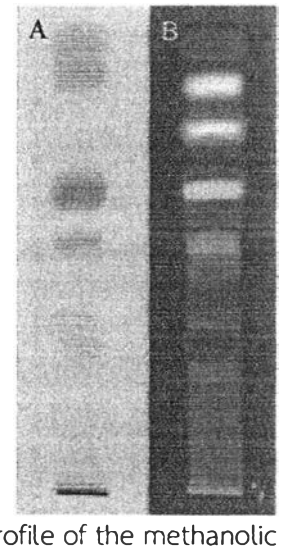

Figure 18. TLC profile of the methanolic heartwood extract of AM visualized at (A) 254 and (B) 366 nm

Activity-guided fractionation was carried out by isolating each band/fraction separated on the PLC silica gel 60 F_{254} glass plate and were tested for the 5α-R1 inhibitory activity.

4.9 Activity-guided fractionation of *Avicennia marina*

Activity-guided fractionation was carried out by isolating the bands/fractions from the PLC plates through a simple technique of scratching. The bands/fractions were re-spotted on TLC Silica gel 60 F_{254} aluminum plate and developed using toluene: acetonitrile: ethyl acetate: acetic acid in the ratio of 7:1:3:0.03 as the mobile phase **(Figure 19).**

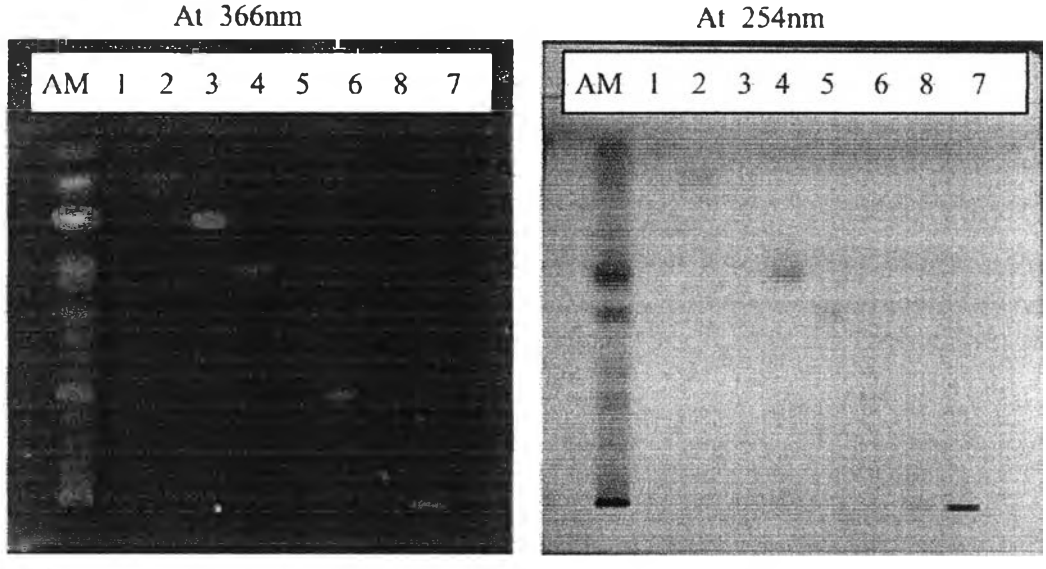

Figure 19. TLC plate visualized at 366 and 254nm showing the isolated bands/fractions

The bands/fractions were then tested for the 5α-R1 inhibitory activity using the optimized assay system **(Figure 20).** The concentration of 10 µg/ml was taken as the upper limit and the final concentrations of all the bands/fractions for the activity test as the AM extract possessed toxicity above this concentration **(Figure 12B).**

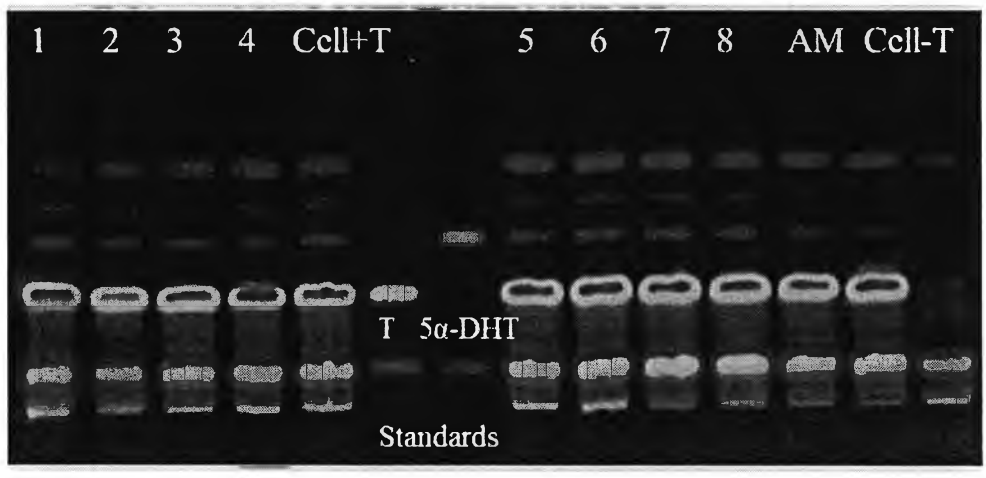

Figure 20. Results on the 5α-R1 inhibitory activity of the bands/fractions numbered 1-8 and AM in HHDPC-based assay system using non-radioactive TLC detection technique. The internal (Cell+T) and negative (Cell-T) controls are shown in the middle and the right-hand side of the plate, respectively.

It can be clearly seen in **Figure 20** that fraction '4' exhibited similar 5α-R1 inhibitory activity compared to that of the methanolic crude extract of AM with an IC_{50} value of 9.80 µg/ml **(Figures 21)**.

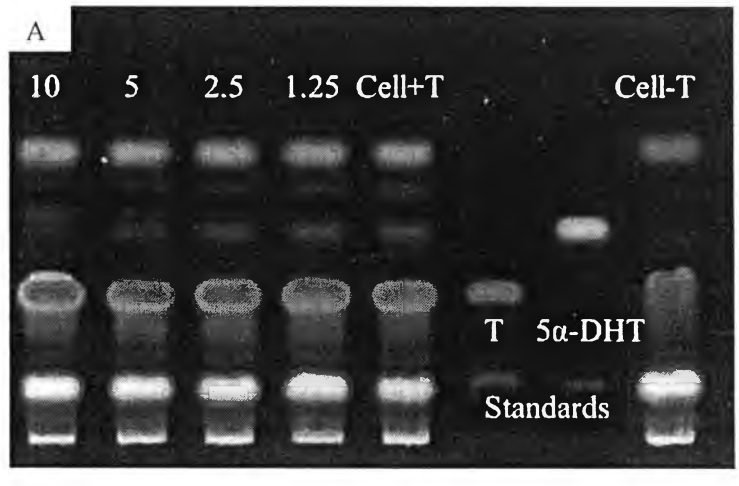

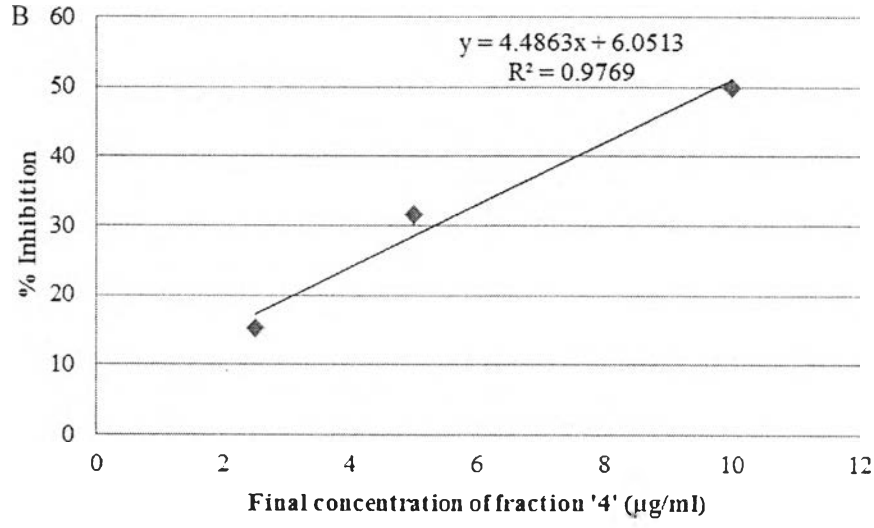

Figure 21. (A) TLC plate showing 5α-R1 inhibitory activity of fraction '4' at 10, 5, 2.5 and 1.25 µg/ml. The internal control (Cell+T) and negative control (Cell-T) are shown in the middle and right-hand side of the plate, respectively. (B) IC_{50} curve of fraction '4'

Fraction '4' is a mixture of atleast 3 compounds which were seen in green and blue colors at 366nm **(Figure 19)**, hence labeled as B1, G1 and B2 (from top-down). Separation of the 3 compounds was conducted on the PLC Silica gel 60 F_{254} glass plate through double development in toluene: acetonitrile in the ratio of 8:2 as the mobile phase. The isolates were re-spotted on TLC Silica gel 60 F_{254} aluminum plate using the same system **(Figure 22)**.

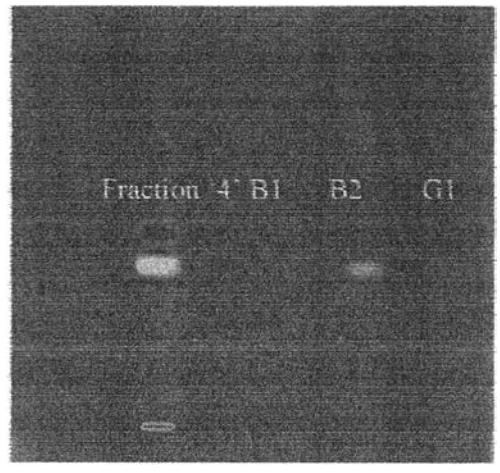

Figure 22. Isolated B1, B2 and G1 from fraction '4' through double developing the TLC plate in toluene: acetonitrile in the ratio of 8:2

The 3 compounds and their combinations of B1B2, B1G1, B2G1 and B1B2G1 in equal amounts were again tested for the 5α-R1 inhibitory activity. As shown in **Figure 23A and 23B**, only G1 alone showed similar 5α-R1 inhibitory activity as AM and fraction '4' with an IC_{50} of 9.94 μg/ml **(Figures 24)**. Therefore, anti-androgenic activity of G1 was evaluated at the upper limit of 10 μg/ml as the final concentration.

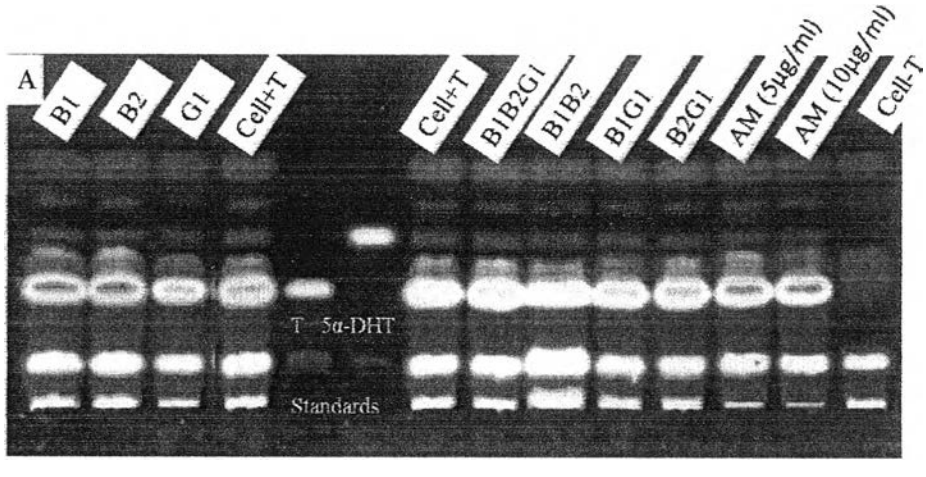

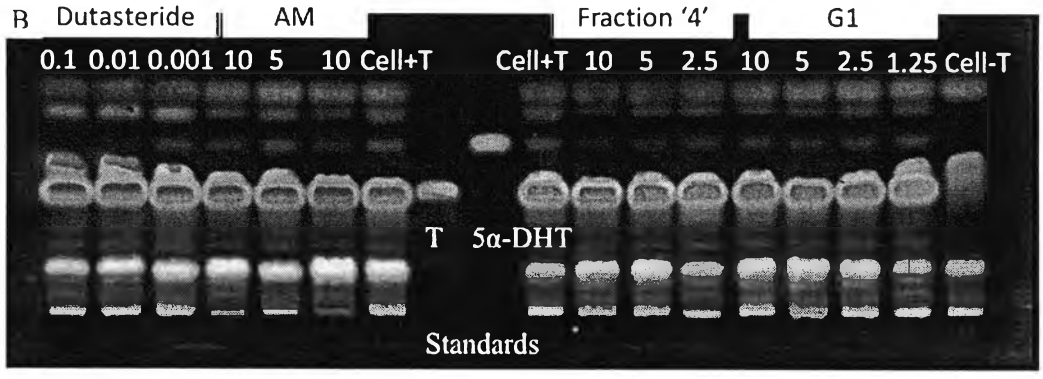

Figure 23. Results on the 5α-R1 inhibitory activity of (A) B1, B2, G1, B1B2G1, B1B2, B1G1, B2G1 and AM at 10 µg/ml (B) Dutasteride, AM, fraction '4' and G1 at the indicate final concentrations in µg/ml. The internal (Cell+T) and negative (Cell-T) controls are shown in the middle and right-hand side of the plate, respectively.

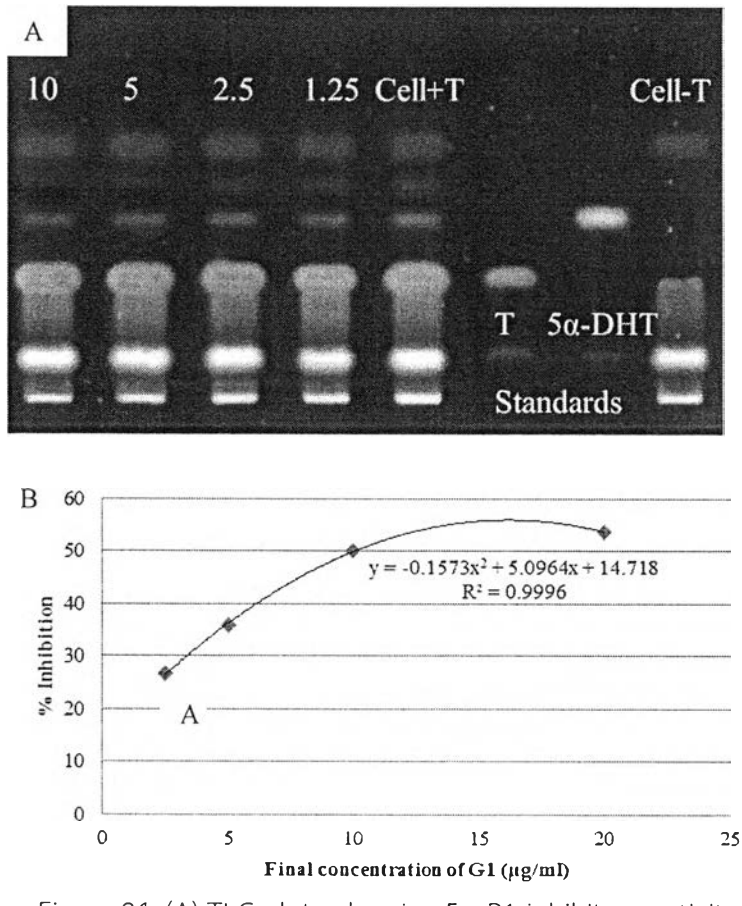

Figure 24. (A) TLC plate showing 5α-R1 inhibitory activity of G1 at 10, 5, 2.5 and 1.25 µg/ml. The internal control (Cell+T) and negative control (Cell-T) are shown in the middle and right-hand side of the plate, respectively. (B) IC_{50} curve of G1

4.10 Anti-androgenic activity of the 5α-reductase inhibitory compound(s)

As G1 alone exhibited 5α-R1 inhibitory activity similar to the methanolic crude extract of AM, therefore its anti-androgenic activity was also tested. As shown in **Figure 25**, G1 only up-regulated the expression of VEGF from 0.666 to 0.727 in presence of 10^{-4} M T (lane 5 compared to lane 2, Figure 25) and from 0.401 to 0.763 in presence of 10^{-4} M 5α-DHT (lane 6 compared to lane 3, Figure 25). G1 alone did not affect the expression of VEGF (lane 4 compared to lane 1, Figure 25). However, G1 alone (lane 4 compared to lane 1, Figure 25) or in presence of 10^{-4} M T (lane 5 compared to lane 2, Figure 25) and 10^{-4} M 5α-DHT (lane 6 compared to lane 3, Figure 25) down-regulated the expression of FGF-7 from 1 to 0.712, 0.860 to 0.677 and 0.746 to 0.600, respectively. The negative effect of AM **(Figure 16)** on the expression of HGF was not observed with G1 (lane 4 compared to lane 1, Figure 25) while an additional overcoming effect on the expression of HGF was observed in presence of 10^{-4} M T from 0 to 0.380 (lane 5 compared to lane 2, Figure 25). Statistically, G1 did not significantly up-regulate the expression of VEGF as the crude extract of AM but still exhibited 5α-R1 inhibitory activity.

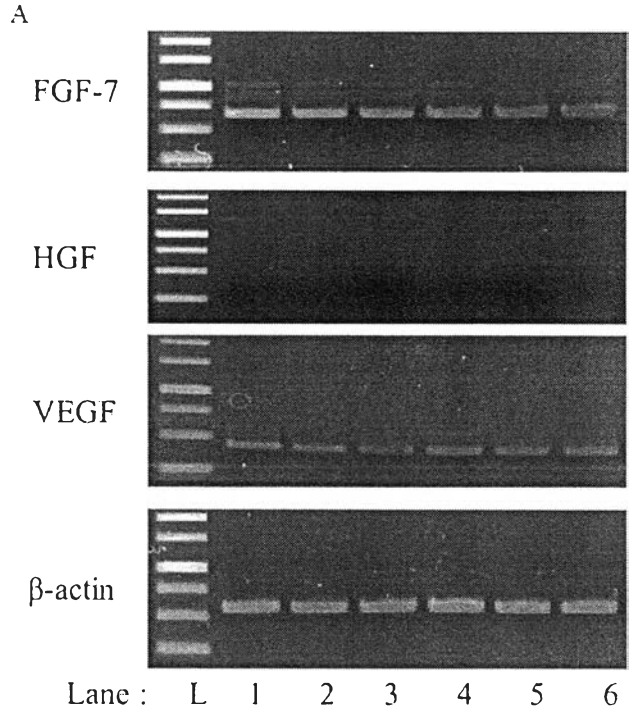

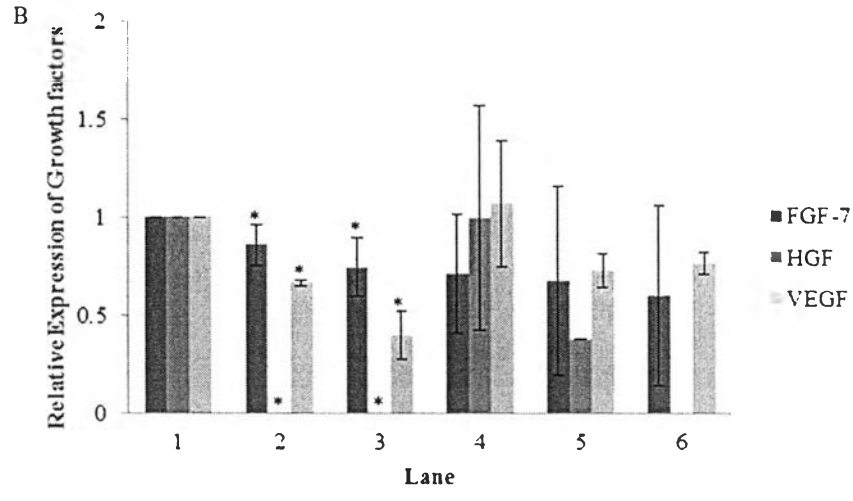

Figure 25. (A) RT-PCR and (B) relative levels of the mRNA expression of growth factors from androgens and G1 treated and un-treated HHDPCs. Growth factors include FGF-7 (fibroblast growth factor-7, 653 bp), HGF (hepatocyte growth factor, 1320 bp) and VEGF (vascular endothelial growth factor, 440 bp) while β-actin (584 bp) was used as an internal control. The 1-kb DNA ladder shows the sizes of 2, 1.5, and 1 kb and 750, 500 and 250 bp from top-down (lane L) and HHDPC treated with 1% DMSO (Lane 1), 10^{-4} M T (Lane 2), 10^{-4} M 5α-DHT (Lane 3), 10 µg/ml of G1 (Lane 4), 10 µg/ml of G1 and 10^{-4} M T (Lane 5) and 10 µg/ml of G1 and 10^{-4} M 5α-DHT (Lane 6). *- statistically significant compared to lane 1 ($p<0.05$).

This result suggested that the significant up-regulation of VEGF might be due to the synergistic effect of other compounds presented in fraction '4' from which G1 was isolated. Therefore, anti-androgenic activity of fraction '4' was also conducted **(Figure 26)**. In presence of 10^{-4} M T, fraction '4' up-regulated the expression of FGF-7 and VEGF from 0.869 to 0.960 and from 0.277 to 1.00 (lane 5 compared to lane 2, Figure 26), respectively. A similar effect was observed in presence of 10^{-4} M 5α-DHT, where FGF-7 was up-regulated from 0.712 to 0.960 and VEGF from 0.247 to 1.07 (lane 6 compared to lane 3, Figure 26). Fraction '4' itself did not have any effect on the expression of FGF-7 and VEGF, however, it down-regulated the expression of HGF from 1 to 0.501 (lane 4 compared to lane 1, Figure 26). This result was similar when the cells were treated with AM alone. Fraction '4' exhibited the down-regulation of

HGF in presence of 10^{-4} M T from 0.270 to 0.168 (lane 5 compared to lane 2, Figure 26) while a minimal up-regulation was observed in presence of 10^{-4} M 5α-DHT from 0 to 0.105 (lane 6 compared to lane 3, Figure 26). Statistically, fraction '4' significantly up-regulated the expression of VEGF in androgen-treated HHDPCs while exhibiting down-regulation of HGF in un-treated HHDPCs.

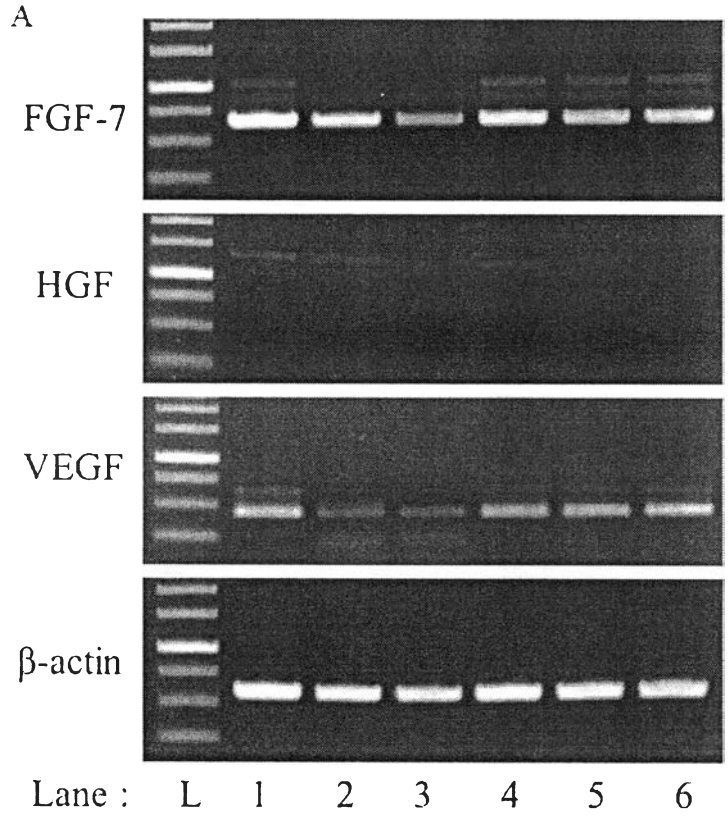

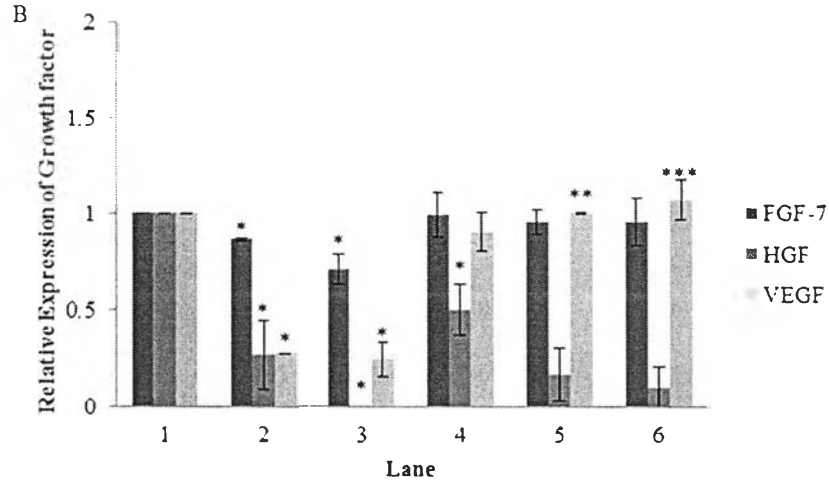

Figure 26. (A) RT-PCR and (B) relative levels of the mRNA expression of growth factors from androgens and fraction '4' treated and un-treated HHPDCs. Growth factors include FGF-7 (fibroblast growth factor-7, 653 bp), HGF (hepatocyte growth factor, 1320 bp) and VEGF (vascular endothelial growth factor, 440 bp) while β-actin (584 bp) was used as an internal control. The 1-kb DNA ladder shows the sizes of 2, 1.5, and 1 kb and 750, 500 and 250 bp from top-down (lane L) and HHDPC treated with 1% DMSO (Lane 1), 10^{-4} M T (Lane 2), 10^{-4} M 5α-DHT (Lane 3), 10 µg/ml of fraction '4' (Lane 4), 10 µg/ml of fraction '4' and 10^{-4} M T (Lane 5) and 10 µg/ml of fraction '4' and 10^{-4} M 5α-DHT (Lane 6). *- statistically significant compared to lane 1, **- statistically significant compared to lane 2, ***- statistically significant compared to lane 3 ($p<0.05$)

From all the results obtained, it can be concluded that AM and fraction '4' both exhibited 5α-R1 inhibitory and anti-androgenic activities while G1 possess only 5α-R1 inhibitory activity. Structure elucidation of G1 was conducted using ^{1}H-NMR and ^{13}C-NMR.

4.11 Structure elucidation of G1

G1 obtained from the PLC Silica gel 60 F_{254} glass plate was check for its purity using analytical HPLC Capcell pak ODS (0.46x 25 cm, 5 µm) column at the flow rate of 1 ml/min in the mobile phase of 90% acetonitrile in water and was detected using UV-Vis detector at 205 nm **(Figure 27A)**. It was observed that there were contaminations in the isolate of G1 and therefore, it was subjected to re-purification using semi-preparative HPLC. The separation of G1 was achieved through the

application of 45mg of the mixture in 450 µl of DMSO to TSK gel ODS (2x25 cm, 5 µm) column using 30% acetonitrile as a mobile phase with a flow rate of 9 ml/min. The compounds isolated were detected at 205 nm using 875-UV UV-Vis detector and recorded on SS-250F. The HPLC chromatogram **(Figure 27B)** showed that there are three major peaks which were referred as G1.3 (0.9mg), G1.5 (1.6mg) and G1.7 (3.9mg).

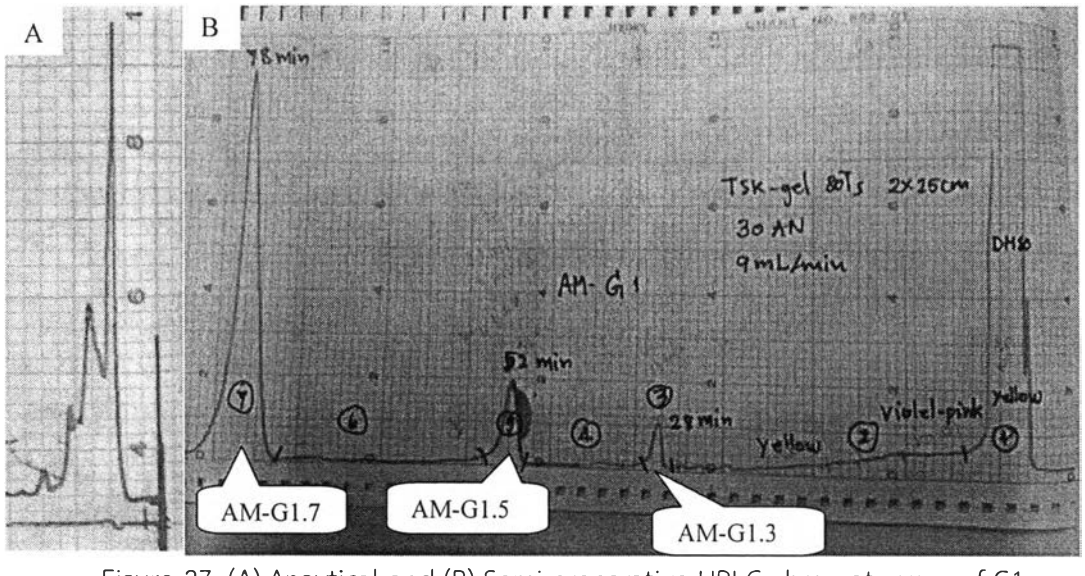

Figure 27. (A) Anaytical and (B) Semi-preparative HPLC chromatogram of G1

All the three isolates were re-spotted on the TLC Silica gel 60 F_{254} aluminum plate and was developed once in toluene: acetonitrile in the ratio of 8:2. It was found that G1.7 is G1 which exhibited 5α-R1 inhibitory activity **(Figure 28)** and therefore, structure elucidation of this unknown compound was carried out using ^{1}H-NMR and ^{13}C-NMR in deuterated trichloromethane ($CDCl_3$).

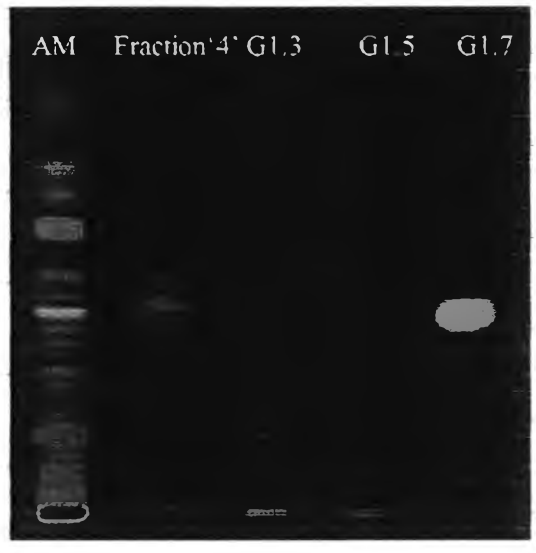

Figure 28. TLC plate developed in toluene: acetonitrile in the ratio of 8:2 and visualized at 366nm showing AM, fraction '4', G1.3, G1.5 and G1.7

A

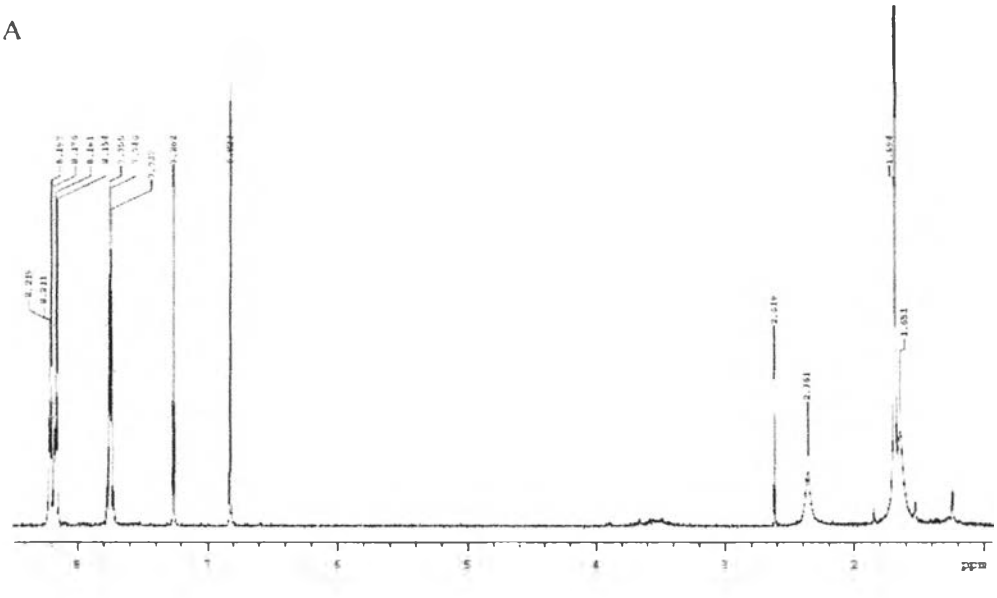

B

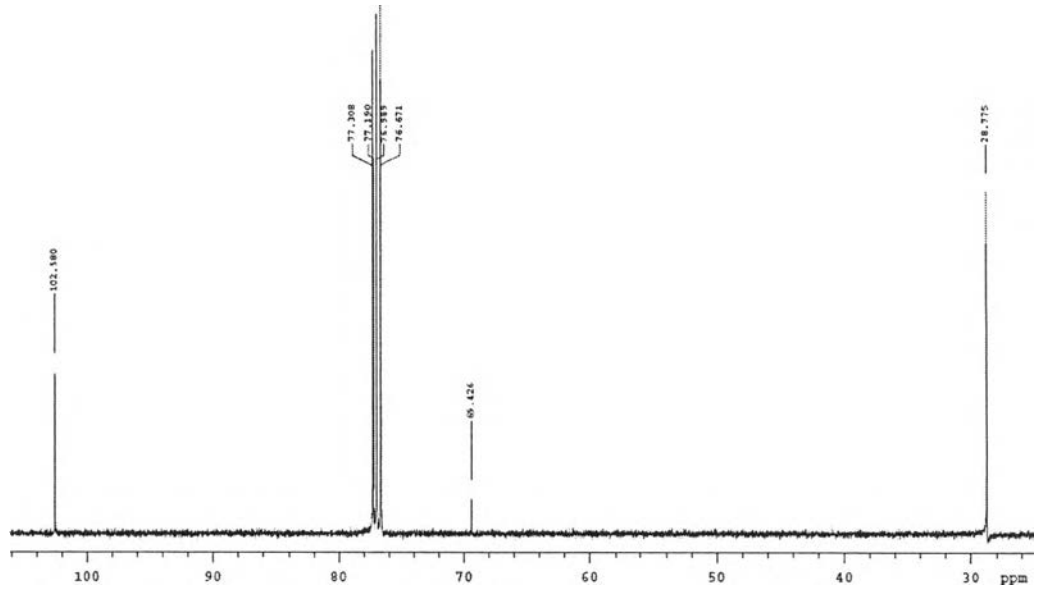

C

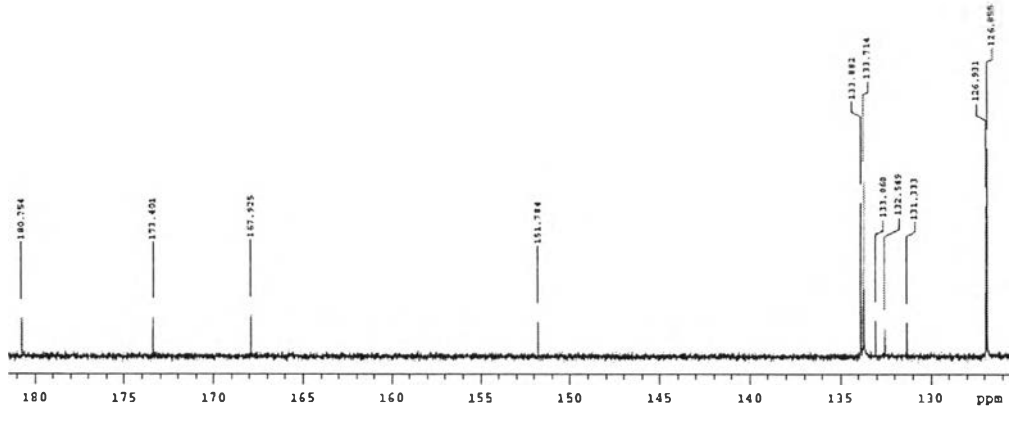

Figure 29 (A) ^{1}H-NMR and (B-C) ^{13}C-NMR spectra of G1

The NMR spectra **(Figures 29)** indicates the chemical shift value, a characteristic of NMR represented in parts per million (ppm) (x-axis), of each proton (H) and carbon (C) in different chemical environment within the unknown structure. Therefore, these values were used to identify the structure of G1.

The ^{1}H-NMR and ^{13}C-NMR spectrum in $CDCl_3$ of G1 showed four contiguous aromatic proton at δ 8.21 (1H, m), 8.16 (1H, m) and 7.75 (2 H, m) assignable to two deshielded protons (H-5, H-8) *peri*-located to two carbonyl groups and other two aromatic protons (H-6, H-7), respectively. In addition, two typical carbonyl carbon signal at δ 173.3 (C-1) and 180.8 (C-4) indicated the 1, 4-naphthoquinone nucleus with no substituent on aromatic ring. The low field signal at δ 69.4 (C-3′) indicated oxygen-attached quaternary carbon of 1-hydroxy-1-methylethyl prenylated side-chain with a sharp singlet at δ 1.69 (6H, H-4′, H-5′) assignable to two prenylated methyls. A singlet proton at δ 6.82 (1H, s, H-1′) and carbon signal at δ 102.6 was also observed.

Based on the above spectral evidence and comparison with previously reported ^{1}H-NMR and ^{13}C-NMR datas [61, 62] **(Table 9)**, G1 was identified as naphtho [2,3-β]furan-1,4-dione, 2'-(1-hydroxy-1-mehtylethyl) or Avicequinone C **(Figure 30)** with a molecular formula of $C_{15}H_{12}O_4$ and a molecular weight of 256.

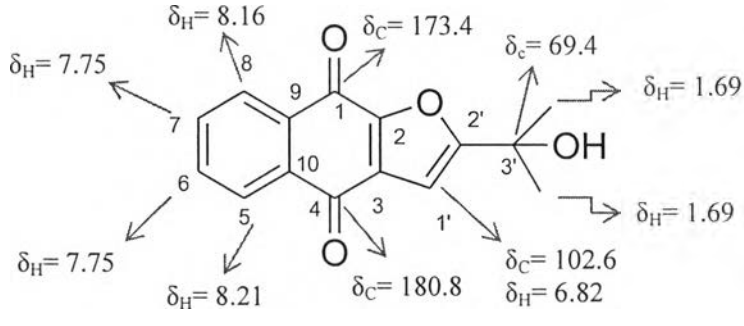

Figure 30. Structure of Avicequinone C

The 5α-R1 inhibitory activity of Avicequinone C with an IC_{50} of 38.8 µM might be due to the 2 carbonyl groups presented in the 1,4 naphthoquinone nucleus as it does in alizarin, which exhibited 5α-R1 in cell-free and cell-based assay with an IC_{50} of 3 and 6 µM, respectively [19].

Table 9

NMR spectral datas of G1 and Avicequinone C in $CDCl_3$

Position	G1		Avicequinone C [61, 62]	
	^{1}H(mult., J in Hz)	^{13}C	^{1}H(mult., J in Hz)	^{13}C
1	-	173.4	-	173.3
2	-	151.8	-	151.6
3	-	131.3	-	131.2
4	-	180.8	-	180.7
5	8.16 (m)	126.9	8.14 (m)	126.8
6	7.75(m)	133.9	7.73(m)	133.9
7	7.75(m)	133.7	7.73(m)	133.7
8	8.21(m)	126.8	8.18(m)	126.8
9	-	132.5	-	132.4
10	-	133.1	-	
1'	6.82(s)	102.6	6.80(s)	102.6
2'	-	167.9	-	168.1
3'	-	69.4	-	69.3
4'	1.69(s)	28.8	1.67(s)	28.7
5'	1.69(s)	28.8	1.67(s)	28.7

4.12 Structure elucidation of B2

Structure elucidation of one of the unknown compound, B2, in fraction '4' was conducted as it possesses synergistic anti-androgenic activity. In order to do so, first the B2 obtained from PLC Silica gel 60 F_{254} glass plate were checked for its purity using analytical HPLC Capcell pak ODS (0.46x 25 cm, 5 µm) column at the flow rate of 1 ml/min in 50% and 60% acetonitrile in water and was detected using UV-Vis detector at 205 nm **(Figure 31)**.

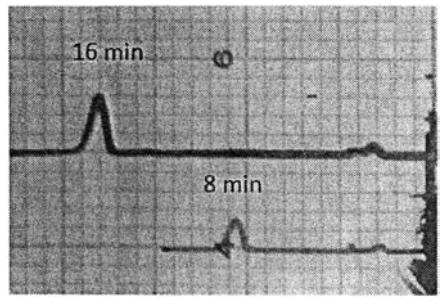

Figure 31. Analytical HPLC chromatogram of B2

The ^{1}H-NMR and ^{13}C-NMR spectrum in $CDCl_3$ of B2 **(Figures 32)** showed four aromatic proton as an AA′BB′ system at δ 8.05 (1H, d, J = 9.6 Hz, H-5), 8.02 (1H, m d, J = 10 Hz, H-8), 7.43 (1H, d, J = 7.6 Hz, H-6) and 7.33 (1H, d, J = 7.6 Hz, H-7) were assigned in ring A. The signals at δ 3.99 and 4.03 (3H, s, each) were attributed to the methoxyl groups at C-1 and C-4 in ring B, respectively, from the HMQC and HMBC spectra. These data indicated a 1, 4-dimethoxynaphthol skeleton. The proton signals at δ 3.40 (2H, d, J = 8.4 Hz, H-1′) and oxygenated proton 4.73 (H, t, J = 8.4 Hz, H-2') couple to each other of furan ring were observed. Moreover the C-H long range correlation of the carbon at δ 147.3 (C-2) with δ 3.40 (H-2') suggested the attachment of furan ring to ring B. The presence of two 3H singlets at δ 1.28 and 1.42, a quaternary carbon at δ 71.8 (C-3′) were indicated to 2′-isopropanol, which showed correlation in the HMBC spectrum.

The molecular formula of $C_{17}H_{20}O_4$ was deduced from the HRESIMS at *m/z* 311.1287 $[M+Na]^+$ (cald 311.1259 for $C_{17}H_{20}NaO_4$) **(Figure 33)**. Base on the above spectral evidence and comparison with previously reported ^{1}H and ^{13}C-NMR datas [61], B2 was identified as 1,4-naphthoquinol, naphtha [2,3-β] furan-1,4-dimethoxy, 2′-(1-hydroxy-1-mehtylehtyl) or Avicenol C **(Figure 34)**. The relative stereochemistry of B2 was determined by a NOESY experiment, in which the NOE correlations between H-1′ and 1′-OC<u>H</u>$_3$ (δ 3.99) H-2′ and CH_3-5′ and between H2′ and CH_3-5′. Thus, H-1′, H-2′ and CH_3-5′ were suggested to be located in a β-orientation **(Figure 35)**.

A

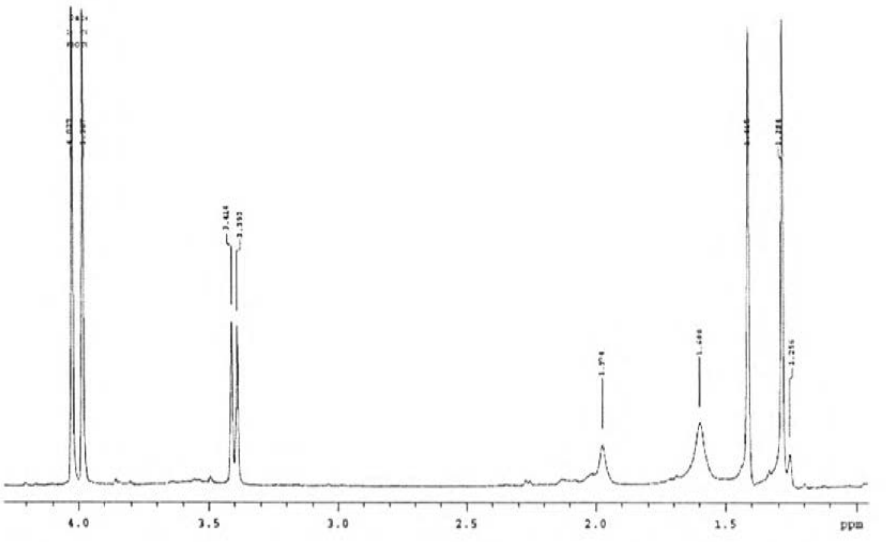

B

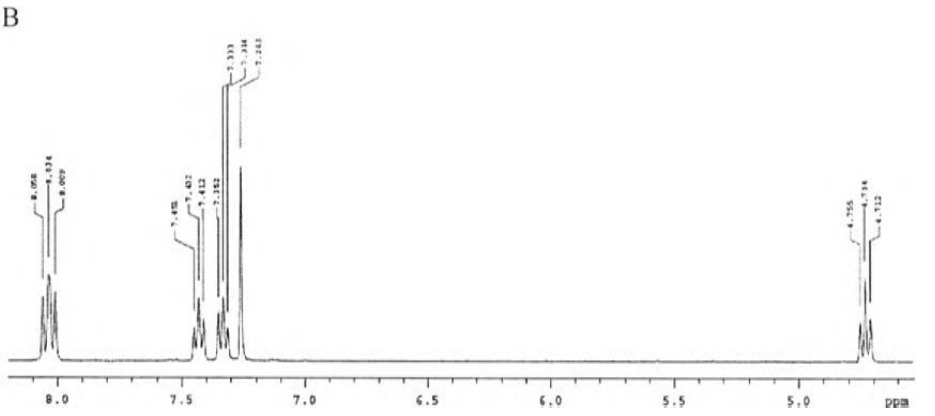

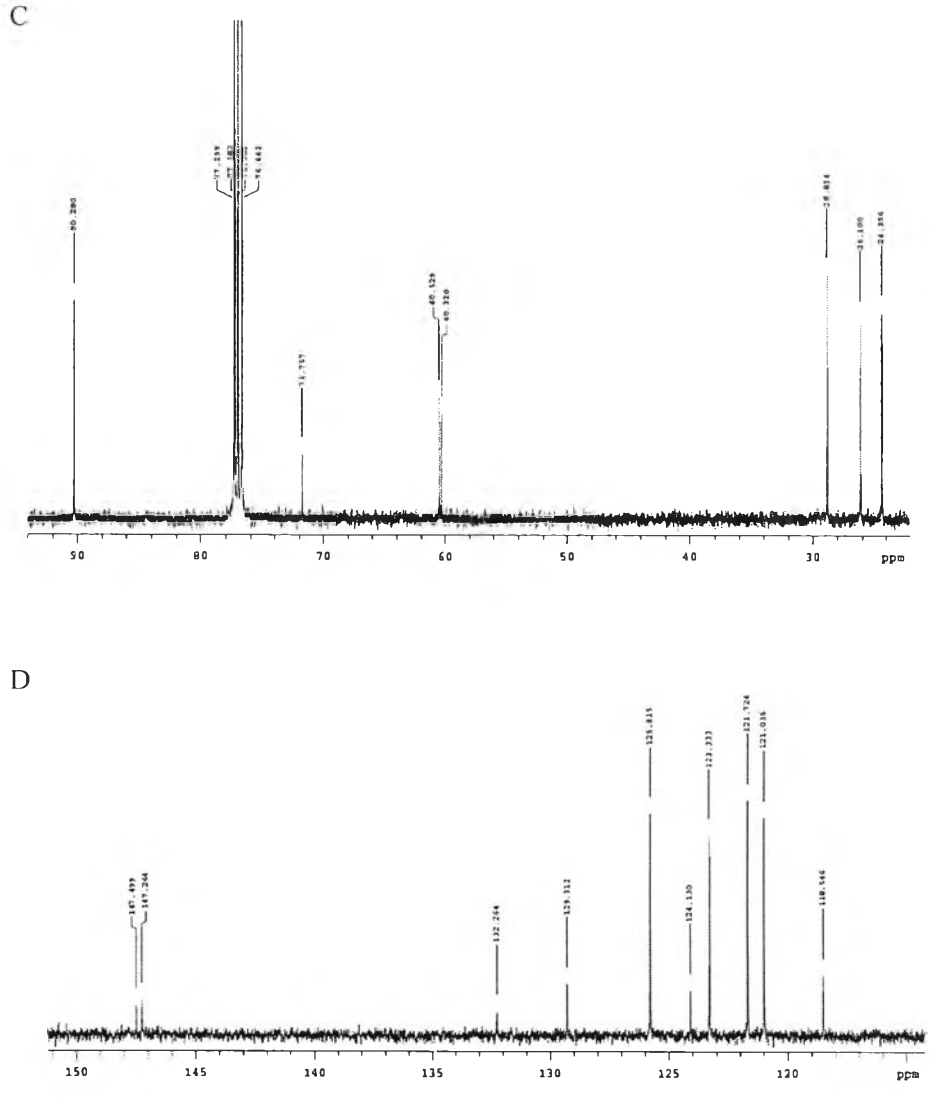

Figure 32. (A-B) ^{1}H-NMR and (C-D) ^{13}C-NMR spectra of B2

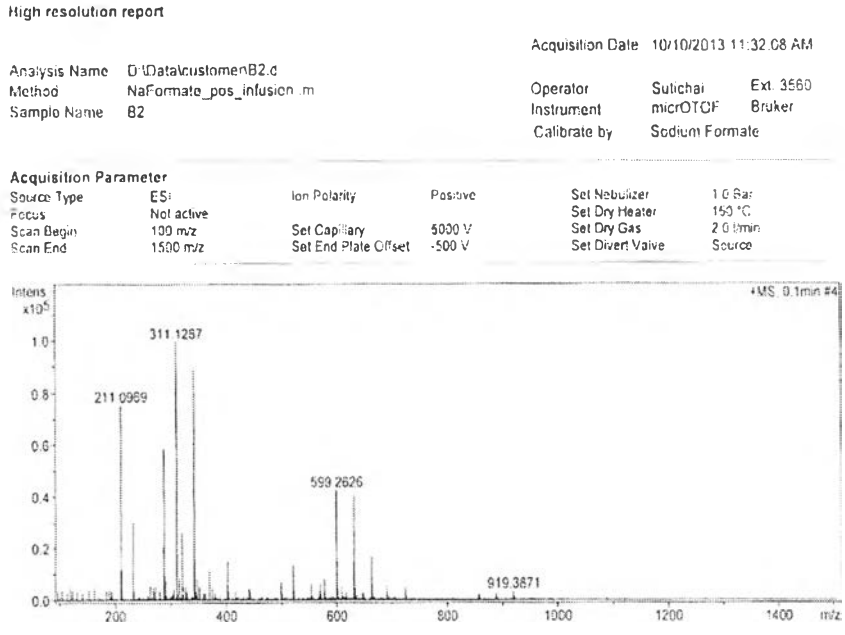

Figure 33. HRESIMS spectrum of B2

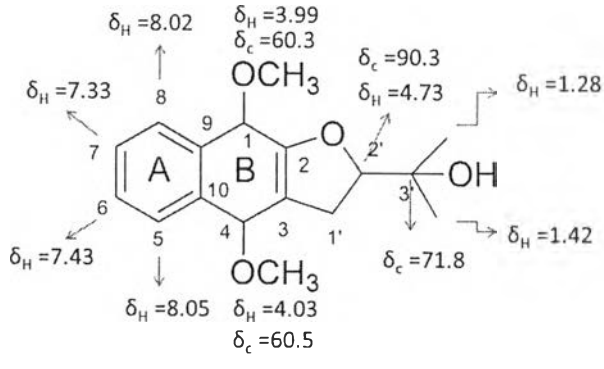

Figure 34. Structure of Avicenol C

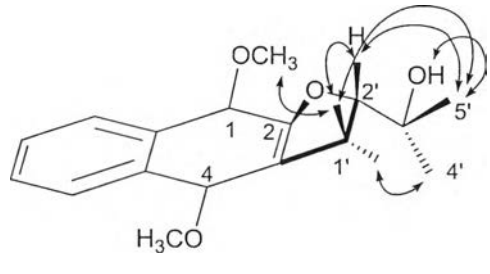

Figure 35. β-orientation of Avicenol C based on the NOESY data

Table 10

NMR spectral datas of B2 and Avicenol C in $CDCl_3$

Position	B2			Avicenol C [61]	
	^1H (mult., *J* in Hz)	^{13}C	HMBC (correlation with ^1H)	^1H (mult., *J* in Hz)	^{13}C
1	-	147.5	H-1', 1'-OCH_3	-	147.5
2	-	147.3	H-8, H-1', 1'-OCH_3	-	147.2
3	-	118.5	H-1'	-	118.5
4	-	132.3	4'-OCH_3, H-5	-	132.2
5	8.05(br d, 9.6)	129.3	H-6, H-8	8.02(br d, 8.4)	129.3
6	7.43(br t, 7.6)	121.0	H-7	7.41(br t, 8.4)	121.0
7	7.33(br t, 7.6)	125.8	H-8	7.31(br t, 8.4)	125.8
8	8.02(br d, 10)	123.3	H-5	8.00(br d, 8.4)	123.3
9	-	121.7	H-6	-	121.7
10	-	124.3	H-7	-	124.1
1'	3.40(d, 8.4)	28.3	-	3.38(d, 8.4)	28.8
2'	4.73(t, 8.4)	90.3	H-4', H-5', H-1'	4.71(t, 8.4)	90.3
3'	-	71.8	H-4', H-5', H-1'	-	71.7
4'	1.28(s)	24.4	H-2', H-3', H-5'	1.26(s)	24.3
5'	1.42(s)	26.1	H-2', H-3', H-4'	1.39(s)	26.1
1'-OCH_3	3.99(s)	60.3	H-2	3.96(s)	60.3
4'-OCH_3	4.03(s)	60.5	H-4	4.01(s)	60.6
3'-OH	2.00(br s)		H-5'	1.90(br s)	

Conclusions

AGA is the major type of scalp hair loss which is caused due to the over-production of 5α-DHT, a potent androgen produced within the HHDPCs by the 5α-R [1-6]. Therefore, one possible method of treating AGA is to inhibit this enzymatic reaction. Most of the research works were conducted using irrelevant systems [13-19] and therefore, we have developed an AGA relevant cell-based assay using HHDPCs which are the main regulator of hair growth [1, 9, 22]. The developed assay system combined with non-radioactive TLC detection technique was used to screen forty-one Thai medicinal plant extracts for the 5α-R1 inhibitory activity, the isoform present in HHDPCs. The assay system was validated with a well-known 5α-R1 inhibitor, dutasteride with an IC_{50} of 0.005 µg/ml or 9.7 nM. Among all the extracts screened, it was found that methanolic heartwood extract of *Avicennia Marina* (AM) exhibited the highest inhibitory activity as it reduces the 5α-DHT production by 52% at the final concentration of 10 µg/ml (IC_{50}= 9.21 µg/ml).

It has been well-established that the reduction of 5α-DHT leads to the lowering of receptor-ligand complex formation affecting the induction of androgen-sensitive genes of IGF-1, FGF-7, HGF and VEGF produced by HHDPCs [20-21]. These growth factors induce the proliferation and differentiation of the hair matrix cells to form the other keratinocyte layers of the hair follicle during the anagen phase of the hair cycle, leading to hair growth [23-24]. This effect is known as the anti-androgenic activity of a potential 5α-R inhibitor. Therefore, AM and dutasteride were tested for its potential anti-androgenic activity in presence of androgens and it was found that both AM and dutasteride showed a significant increase in the mRNA expression of VEGF in presence of T. In addition, an increase in the expression of VEGF in presence of 5α-DHT indicated that there are other pathways through which these two compounds interact with HHDPCs.

In order to obtain the active compounds with 5α-R1 inhibitory activity from the methanolic plant extract of AM, activity-guided fractionation was conducted on PLC silica gel 60 F_{254} glass plate. The bands/fractions visualized at 366 nm on the PLC plate were isolated through a simple method of scratching and were tested for the 5α-R1 inhibitory activity. It was found that fraction '4' exhibited a similar inhibitory activity as AM with an IC_{50} of 9.80 µg/ml. Fraction '4' was a combination of B1, G1 and B2. These compounds and their combinations were tested for the 5α-R1 inhibitory activity which resulted in the identification of G1 as an active compound

within the methanolic extract of AM, with an IC_{50} of 9.94 µg/ml or 38.8 µM. G1, identified as Avicequinone C, however, did not exhibit significant increase in the mRNA expression of the growth factors produced by HHDPCs but a significant effect was observed when treated with fraction '4' from which Avicequinone C was isolated. Therefore, the anti-androgenic activity was due to the synergistic effect of B1, Avicequinone C (G1) and Avicenol C (B2).

In this research work, a novel cell-based assay system was established using HHDPCs to screen for new 5α-R1 inhibitors specifically for treating AGA. This assay system was coupled with a non-radioactive TLC detection technique and an active compound from the methanolic heartwood extract of AM was identified as Avicequinone C with potential in treating AGA.